

NASA Contractor Report 165707

Parametric Analytical Studies for the  
Nonlinear Dynamic Response of the  
Tile/Pad Space Shuttle  
Thermal Protection System

Harold Edighoffer

GENERAL ELECTRIC COMPANY  
Re-entry Systems Division  
Philadelphia, PA 19101

Contract NAS1-16121

October 28, 1981



National Aeronautics and  
Space Administration

**Langley Research Center**  
Hampton, Virginia 23665

PARAMETRIC ANALYTICAL STUDIES FOR THE  
NONLINEAR DYNAMIC RESPONSE OF THE  
TILE/PAD SPACE SHUTTLE  
THERMAL PROTECTION SYSTEM

By

Harold Edighoffer  
General Electric Company  
Re-entry Systems Division  
Philadelphia, PA 19101

Contract NAS1-16121

[October 28, 1981]

This paper presents a collection of parametric unidirectional analytical studies of the nonlinear dynamic behavior of the space shuttle tile/pad thermal protection system for imposed sinusoidal and random motions of the shuttle skin and/or applied tile pressure. The analysis accounts for the highly nonlinear stiffening hysteresis and viscous behavior of the pad which joins the tile to the shuttle skin. Sinusoidal and random experimental data are used to confirm the validity of the analysis. With no steady pressure on the tile, the system resonant frequency is very high at low amplitude oscillations and decreases rapidly to a minimum value with increased amplitude. When a steady tile pressure in the outboard direction is superimposed on the oscillating input, the resonant frequency increases to very high values while inboard steady pressures decrease the frequency. The inboard steady pressure decreases the maximum tensile pad stress about five times the amount of the steady pressure applied. On the other hand, outboard steady pressure on the tile results in increased maximum tensile pad stress two times the amount of the applied steady pressure until the steady pressure reaches 6.89 kPa (1.0 psi), which is the point of maximum pad stress. Beyond this value the pad stresses decrease with further increase in outboard steady pressure.

**Page intentionally left blank**

**Page intentionally left blank**

## TABLE OF CONTENTS

	<u>Page</u>
LIST OF FIGURES . . . . .	v
LIST OF TABLES . . . . .	viii
SUMMARY . . . . .	1
INTRODUCTION . . . . .	2
SYMBOLS . . . . .	4
TILE/PAD CONFIGURATION AND MATHEMATICAL MODEL PARAMETERS . . . . .	6
PAD RESPONSE TENSILE STRESS LEVELS . . . . .	11
Oscillating Tile Pressure in the Presence of a Steady Tile Pressure . . . . .	11
Multiple Peak Resonant Frequencies . . . . .	17
Oscillating Substrate in the Presence of Steady Tile Pressure . . . . .	21
VARIATION OF NONLINEAR RESPONSE WITH EXCITATION AMPLITUDE . . . . .	27
Pad Maximum Stress . . . . .	27
Tile Resonant Frequency . . . . .	29
Maximum Magnification Factor . . . . .	31
VARIATION OF NONLINEAR RESPONSE WITH TILE STEADY DIFFERENTIAL PRESSURE . . . . .	33
NONLINEAR RANDOM RESPONSE AND PAD MATERIAL CONDITIONING EFFECTS . . . . .	38
Comparison of Linear and Nonlinear Predicted Probability of Occurrence for Positive Peak Pad Stresses Due to Random Gaussian Substrate Acceleration . . . . .	38
Sensitivity of Analytical Prediction to Pad Material Conditioning . . . . .	47

TABLE OF CONTENTS (CONT'D.)

	<u>Page</u>
Comparison of Test and Nonlinear Analysis for Random RMS and Peak Output/Input Acceleration . . . . .	51
TILE MASS EFFECTS . . . . .	53
CONCLUDING REMARKS . . . . .	57
REFERENCES . . . . .	60
APPENDIX	
EFFECT OF LOADING/UNLOADING LOOP PARAMETERS . . . . .	A-1

## LIST OF FIGURES

<u>Figure No.</u>		<u>Page</u>
1	Tile, pad and geometry . . . . .	7
2	Loading/unloading paths within a conditioned hysteretic envelope [pad thickness = 0.406 cm (.160 in.)] . . . . .	10
3	Variation of pad tensile stress with frequency of applied sinusoidal pressure in the absence of steady pressure . . . . .	13
4	Variation of pad tensile stress with frequency of applied sinusoidal pressure in the presence of a steady outboard pressure of -6.89 kPa (-1 psi) . . . . .	14
5	Variation of pad tensile stress with frequency of applied sinusoidal pressure in the presence of a steady outboard pressure of -13.8 kPa (-2 psi) . . . . .	15
6	Variation of pad tensile stress with frequency of applied sinusoidal pressure in the presence of a steady inboard pressure of 6.89 kPa (1 psi) . . . . .	16
7	Variation of pad stress with strain and with time during a cycle for steady outboard pressure in the presence of an oscillating pressure at 180 Hz . . . . .	18
8	Variation of pad stress with strain and with time during a cycle for steady outboard pressure in the presence of an oscillating pressure at 120 Hz . . . . .	19
9	Variation of pad stress with strain and with time during a cycle for steady outboard pressure in the presence of an oscillating pressure at 90 Hz . . . . .	20
10	Variation of pad tensile stress with applied sinusoidal substrate frequency in the absence of steady pressure . . . . .	23
11	Variation of pad tensile stress with applied sinusoidal substrate frequency in the presence of a steady outboard tile pressure of -6.89 kPa (-1 psi). . . . .	24

LIST OF FIGURES (CONT'D.)

<u>Figure No.</u>		<u>Page</u>
12	Variation of pad tensile stress with applied sinusoidal substrate frequency in the presence of a steady outboard tile pressure of $\pm 13.8 \text{ kPa}$ ( $\pm 2.0 \text{ psi}$ ) . . . . .	25
13	Variation of pad tensile stress with applied sinusoidal substrate frequency in the presence of a steady inboard tile pressure of $6.89 \text{ kPa}$ ( $1.0 \text{ psi}$ ) . . . . .	26
14	Variation of pad maximum stress with input amplitude . . . . .	28
15	Variation of tile resonant frequency with input amplitude . . . . .	30
16	Variation of maximum magnification factor with input amplitude . . . . .	32
17	Variation of pad maximum stress with magnitude of tile steady pressure in the presence of oscillating pressure . . . . .	34
18	Variation of pad maximum stress with magnitude of tile steady pressure in the presence of substrate oscillating acceleration . . . . .	35
19	Variation of magnification factor with magnitude of tile steady pressure in the presence of oscillating pressure. . . . .	36
20	Variation of maximum magnification factor with magnitude of tile steady pressure in the presence of substrate oscillation . . . . .	37
21	Comparison of Rayleigh and nonlinear probability distribution predictions for peak positive pad stress (Heavy tile - $1 \text{ g}^2/\text{Hz.}$ ) . . . . .	40
22	Comparison of Rayleigh and nonlinear probability distribution predictions for peak positive pad stress (Heavy tile - $2 \text{ g}^2/\text{Hz.}$ ) . . . . .	41
23	Comparison of Rayleigh and nonlinear probability distribution predictions for peak positive pad stress (Heavy tile - $3.2 \text{ g}^2/\text{Hz.}$ ) . . . . .	42

LIST OF FIGURES (CONT'D.)

<u>Figure No.</u>		<u>Page</u>
24	Comparison of Rayleigh and nonlinear probability distribution predictions for peak positive pad stress (Heavy tile - $6 \text{ g}^2/\text{Hz.}$ ) . . . . .	43
25	Comparison of Rayleigh and nonlinear probability distribution predictions for peak positive pad stress (Heavy tile - $13 \text{ g}^2/\text{Hz.}$ ) . . . . .	44
26	Comparison of Rayleigh and nonlinear probability distribution predictions for peak positive pad stress (Medium weight tile - $13 \text{ g}^2/\text{Hz.}$ ) . . . . .	45
27	Comparison of Rayleigh and nonlinear probability distribution predictions for peak positive pad stress (Light weight tile - $13 \text{ g}^2/\text{Hz.}$ ) . . . . .	46
28	Sensitivity of tile resonant frequency in the absence of steady tile pressure to pad material conditioning factor, $f_\epsilon$ . . . . .	48
29	Sensitivity of tile peak magnification factor to pad material conditioning factor, $f_\epsilon$ . . . . .	49
30	Sensitivity of tile resonant frequency in the presence of steady tile pressure to pad material conditioning factor, $f_\epsilon$ . . . . .	50
31	Comparison of test and nonlinear analysis for rms and peak acceleration . . . . .	52
32	Effect of tile mass on pad stress for oscillating pressure of $4.785 \text{ kPa}$ (.694 psi) . . . . .	54
33	Effect of tile mass on tile resonant frequency . . . . .	55
34	Variation of pad stress multiplying factor with tile mass . . . . .	56

LIST OF TABLES

<u>Table No.</u>		<u>Page</u>
1	Computer Code Inputs Used / . . . . .	8

## SUMMARY

Parametric analytical studies of the unidirectional nonlinear dynamic behavior of the space shuttle tile/pad thermal protection system is examined for imposed sinusoidal and random motions of the shuttle skin and/or applied tile pressure. Studies are performed using the computer code DYNOTA of Reference 3 which takes into account the highly nonlinear stiffening hysteresis and viscous behavior of the pad joining the tile to the shuttle skin. Where available, experimental data are used to confirm the validity of the analysis. Both analytical and experimental studies reveal that the system resonant frequency is very high for low amplitude oscillations but decreases rapidly to a minimum value with increasing amplitude. Analytical studies indicate that with still higher amplitude the resonant frequency increases slowly. Also, the analysis indicates that in general the tile resonant frequency increases when a steady differential outboard tile pressure is superimposed on the oscillating input and decreases with an inboard pressure. The most important analytical finding is that the maximum response stress in the pad is suppressed five times the imposed steady inward tile pressure applied while the shuttle skin or tile is oscillating at moderate to high oscillating amplitudes. Conversely, the pad stress is increased two times the imposed steady outboard tile pressure up to a steady outboard pressure of about 6.89 kPa (1.00 psi). Because of the nonlinear nature of the system, above 6.89 kPa (1.00 psi) steady outboard pressure, the pad stresses decrease with increasing steady outboard pressure. Obviously, if the space shuttle dynamic environment has its maximum amplitude at a time when there is a 6.89 kPa (1.0 psi) steady outboard tile pressure, it will be more detrimental to the tile/pad system than if the steady tile pressure was inboard.

## INTRODUCTION

The space shuttle orbiter thermal protection system consists of ceramic tiles bonded to thin nylon felt pads, known as strain isolator pads, which are composed of thousands of intertwined nylon filaments. The pads, in turn, are bonded to the aluminum skin (substrate) of the shuttle orbiter.

During a mission, tile/pad combinations experience dynamic loads arising from acoustics, structural vibration, and transonic shock. As a consequence, the pad experiences many cycles of loading of varying magnitudes. Experiments such as those described in reference 1 have shown that as the pad is cyclically loaded and unloaded, hysteresis loops occur in a stress strain characterization of the material. Furthermore, these loops creep as a function of stress level and number of cycles. The creep of the loops eventually becomes very small with each additional cycle, but its effect is to produce a highly nonlinear hardening pad material which is quite soft at low stress levels and considerably stiffer at higher stress levels. As shown in reference 2, for tiles under static loads, the nonlinear pad material properties after cycling significantly affected tile/pad behavior, producing in many cases considerably higher tile/pad through-the-thickness interface stresses than before cycling. The nonlinear pad properties can also be expected to significantly affect the response of the system under dynamic loads.

For a large class of tile/pad combinations (those for which the tile and pad centroids lie along a line normal to the tile surface), a single-degree-of-freedom model of the system is sufficient to characterize the response of the system under uniform applied dynamic pressure or motion. Such a model was developed in reference 3 and can be used to predict dynamic tile/pad through-the-thickness interface stresses which are known to be critical to the integrity of the system.

The purpose of this paper is to present analytical parametric studies and test correlation data for the nonlinear single-degree-of-freedom response of the tile/pad/substrate thermal protection system when subjected to sinusoidal and steady pressure on the tile and/or imposed motion of the substrate. The computer code, DYNOTA , of reference 3 was used to perform this analysis.

The mathematical modeling of the pad material including the assumptions, modeling of the observed stress-strain behavior, damping law, and effective percent of critical damping are all discussed in reference 3.

The following results are presented:

- (1) Variation of pad response tensile stress levels with input frequency.
  - (a) Oscillating tile pressure combined with tile steady pressure.
  - (b) Oscillating substrate combined with tile steady pressure.
- (2) Variation of pad tensile stress with sinusoidal input amplitude.
- (3) Variation of tile resonant frequency with sinusoidal input amplitude.
- (4) Variation of maximum magnification factor with sinusoidal input amplitude.
- (5) Variation of pad maximum stress in the presence of tile steady pressure.
- (6) Variation of maximum magnification factor in the presence of tile steady pressure.
- (7) Comparisons of Rayleigh and nonlinear probability distribution predictions for peak positive pad stress.
- (8) Comparison of random substrate test and nonlinear analysis for rms stress and peak stress.
- (9) Comparison of sinusoidal analysis and test.
  - (a) Tile resonant frequency with substrate acceleration amplitude.
  - (b) Peak magnification with substrate acceleration amplitude.
  - (c) Tile resonant frequency in the presence of steady outboard tile pressure.
- (10) Tile mass effects.
  - (a) Variation of pad stress with tile sinusoidal pressure frequency at a constant amplitude.
  - (b) Variation of tile resonant frequency with tile mass for substrate and tile sinusoidal input.
  - (c) Variation of stress with tile mass for substrate and tile sinusoidal input.

## SYMBOLS

$A_p$	(AREAP)*	pad area
$A_t$	(AREAT)	tile area
$E_L$	(YNGLR)	linear loading modulus
$E_U$	(YNGUL)	linear unloading modulus
$E_S$	—	secant modulus (see equation 1)
$f_\epsilon$	(STRPER)	material strain factor
$f_\sigma$	(DSTRS)	material stress factor
$G$	(GRAV)	gravitational constant
$h_p$	(THICK)	pad thickness
$m$	(SM)	tile mass
$p_1$	(AMPP1)	amplitude of nonoscillatory component of applied tile pressure (positive values act inboard)
$p_2$	(AMPP2)	amplitude of sinusoidal component of applied tile pressure
$q$	(QM)	damping parameter
$w$	(X)	tile displacement
$w_s$	(XBASE)	substrate displacement

\* names enclosed in parentheses are the computer code names in reference 3.

$\ddot{w}$	(A1)	tile acceleration
$z$	—	normal coordinate direction
$\alpha$	, (A1)	substrate acceleration amplitude in g's
$\beta$	(BETA)	secant modulus factor
$\gamma$	(GAMMA)	low stress factor
$\bar{\epsilon}_L$	(CUTOFF 2)	lower cutoff strain
$\bar{\epsilon}_U$	(CUTOFF 1)	upper cutoff strain
$\bar{\epsilon}_{51}$	(EP1)	strain point on pad stress-strain envelope (reference 3)
$\bar{\epsilon}_{61}$	(YP1)	strain point on pad stress-strain envelope (reference 3)
$\epsilon_{\max}$	(ETNMAX)	maximum pad strain when the strain changes from a positive to negative direction
$\epsilon_{\min}$	(ETNMIN)	minimum pad strain when the strain changes from a negative to a positive direction
$\sigma$	(SIG)	pad stress
$\sigma_0$	—	pad stress when the tile has the mass of an LI900 tile
$\sigma_{\max}$	(STNMAX)	maximum pad stress when the strain changes from a positive to negative direction
$\sigma_{\min}$	(STNMIN)	minimum pad stress when the strain changes from a negative to a positive direction
$\zeta$	(DAMP)	damping parameter

## TILE/PAD CONFIGURATION AND MATHEMATICAL MODEL PARAMETERS

The space shuttle tile/pad thermal protection system consists of ceramic tiles bonded to the space shuttle through a nylon felt pad. Reference 3 reported on the development of a unidirectional analysis of the nonlinear dynamic behavior of the pad and an associated computer code. This computer code can be used to perform parametric studies of the tile response when subjected to substrate sinusoidal oscillations and tile sinusoidal pressure oscillations combined with steady differential pressure on the tile.

The values of the tile/pad variables used in performing these studies are tabulated in Table 1. The basic tile/pad configuration selected for this parametric analysis as shown in Figure 1 was a square LI 900 15.24 x 15.24 x 9.525 cm tile on a 12.7 x 12.7 x 0.406 cm pad (6 x 6 x 3.75 in. tile on a 5 x 5 x 0.160 in. pad). This configuration defines the values of pad area, tile area and tile mass given in Table 1. The conditioned pad thickness of .437 cm (.172 in.) was used to represent an original .406 cm (.160 in.) pad thickness. The reasons for selecting the pad property values displayed in Table 1 are given in the Appendix.

As recommended in reference 3, the damping parameters of  $\zeta = 0.15$  and  $q = 2.0$  were used for this parametric evaluation. These values were based on experimental correlation for imposed sinusoidal substrate motion, where the experimental results are presented in reference 4 and 5.

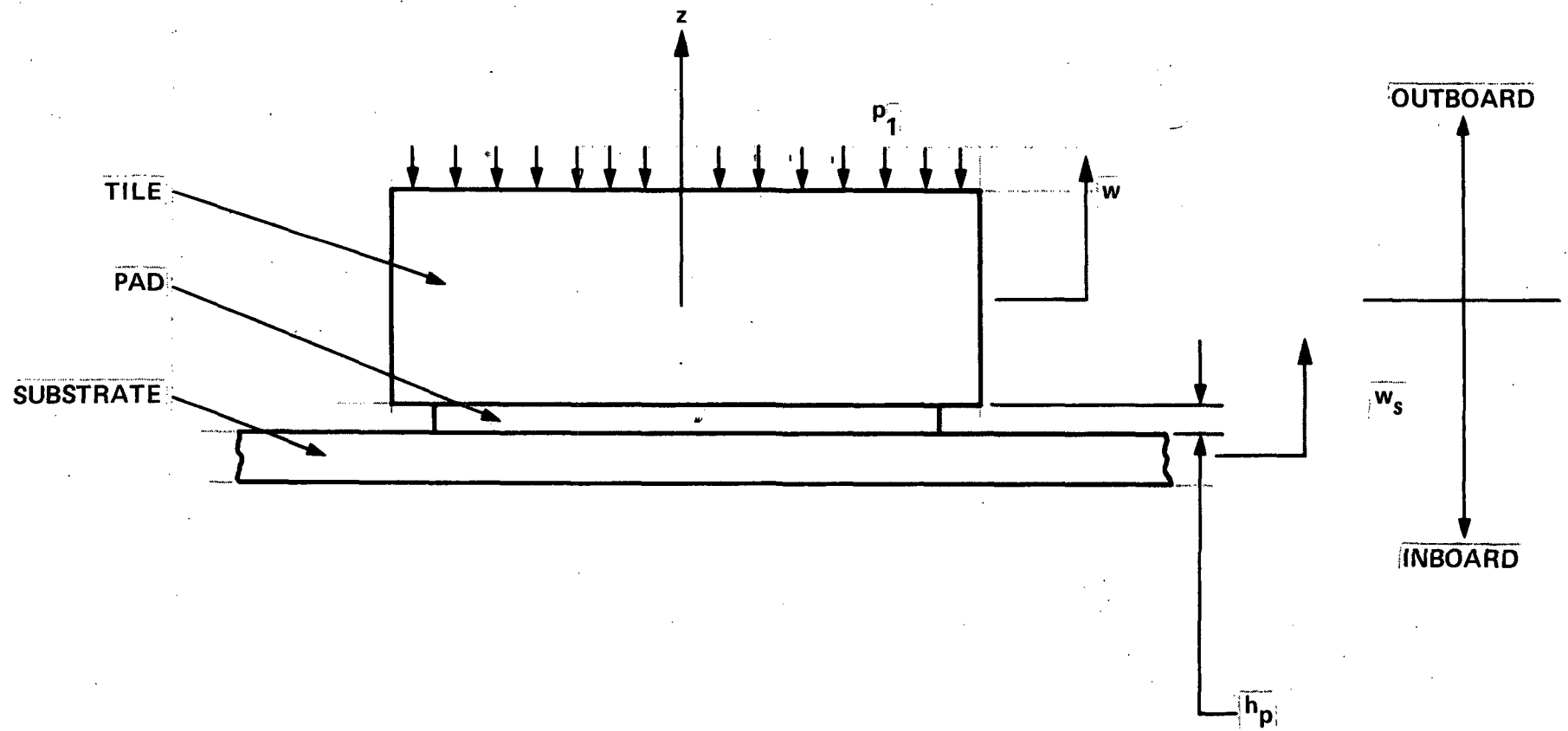


Figure 1. Tile, pad and geometry.

TABLE 1. COMPUTER CODE INPUTS USED

<u>Symbol</u>	<u>Computer Name</u>	<u>Value Used</u>
$A_p$	AREAP	$161.3 \text{ cm}^2$ ( $25 \text{ in}^2$ ) pad area
$A_t$	AREAT	$232.3 \text{ cm}^2$ ( $36 \text{ in}^2$ ) tile area
$h_p$	THICK	.437 cm (.172 in) <sup>*</sup> pad thickness
$m$	SM	.3187 kg (.00182 lb-sec <sup>2</sup> /in) tile mass
$\gamma$	GAMMA	1.0 low stress factor
$\beta$	BETA	100. secant modulus factor
$\epsilon_u^-$	CUTOFF 1	.1744 upper cutoff strain
$\epsilon_l^-$	CUTOFF 2	-.2325 lower cutoff strain
$\zeta$	DAMP	0.15 damping parameter
$q$	QM	2.0 damping parameter
$G$	GRAV	$386 \text{ in/sec}^2$ gravitational constant
$f_\epsilon$	STRPER	1.0 material strain factor
$f_\sigma$	DSTRS	0.0 material delta stress factor

\* The .406 cm (.16 in) pad thickness after conditioning has a thickness of .437 cm (.172 in.)

The pad conditioned stress-strain hysteretic envelope used is shown in Figure 2 and is the envelope defined in reference 1 that was obtained from room temperature static cyclic loading tests reported in reference 1. The upper cut-off strain,  $\bar{\epsilon}_U$ , and the lower cutoff strain,  $\bar{\epsilon}_L$ , are shown in Figure 2 and were set equal to strain values,  $\bar{\epsilon}_{51}$  and  $\bar{\epsilon}_{61}$ , which are the hysteretic envelope transition locations where the path changes from a linear to nonlinear shape as defined in reference 3. This selection results in a curved loading and unloading path in the center portion between  $\bar{\epsilon}_U$  and  $\bar{\epsilon}_L$ . To the right of  $\bar{\epsilon}_U$ , the loading path is linear and the unloading path is curved. To the left of  $\bar{\epsilon}_L$ , the loading path is curved and the unloading path is linear. The curved paths are defined by a fifth order polynomial that results in a shape that is proportional to the outer hysteretic envelope. The equations are presented in reference 3. The computer program keeps track of the maximum pad stress,  $\sigma_{max}$ , and the maximum pad strain,  $\epsilon_{max}$ , when the direction of the strain changes from a positive to a negative direction. In a similar manner the minimum pad stress and strain,  $\sigma_{min}$  and  $\epsilon_{min}$ , are obtained when the strain direction changes from negative to positive. The secant modulus,  $E_S$ , is defined as

$$E_S = \frac{\sigma_{max} - \sigma_{min}}{\epsilon_{max} - \epsilon_{min}} \quad (1)$$

The dashed lines in Figure 2 represent the secant moduli for different equilibrium loops.

To the right of  $\bar{\epsilon}_U$ , the linear loading path is defined as

$$E_L = \beta E_S \quad (2)$$

To the left of  $\bar{\epsilon}_L$ , the linear unloading path is defined as

$$E_U = \beta E_S \quad (3)$$

The appendix contains further discussion of the effect of equation (2) and (3) on the system response.

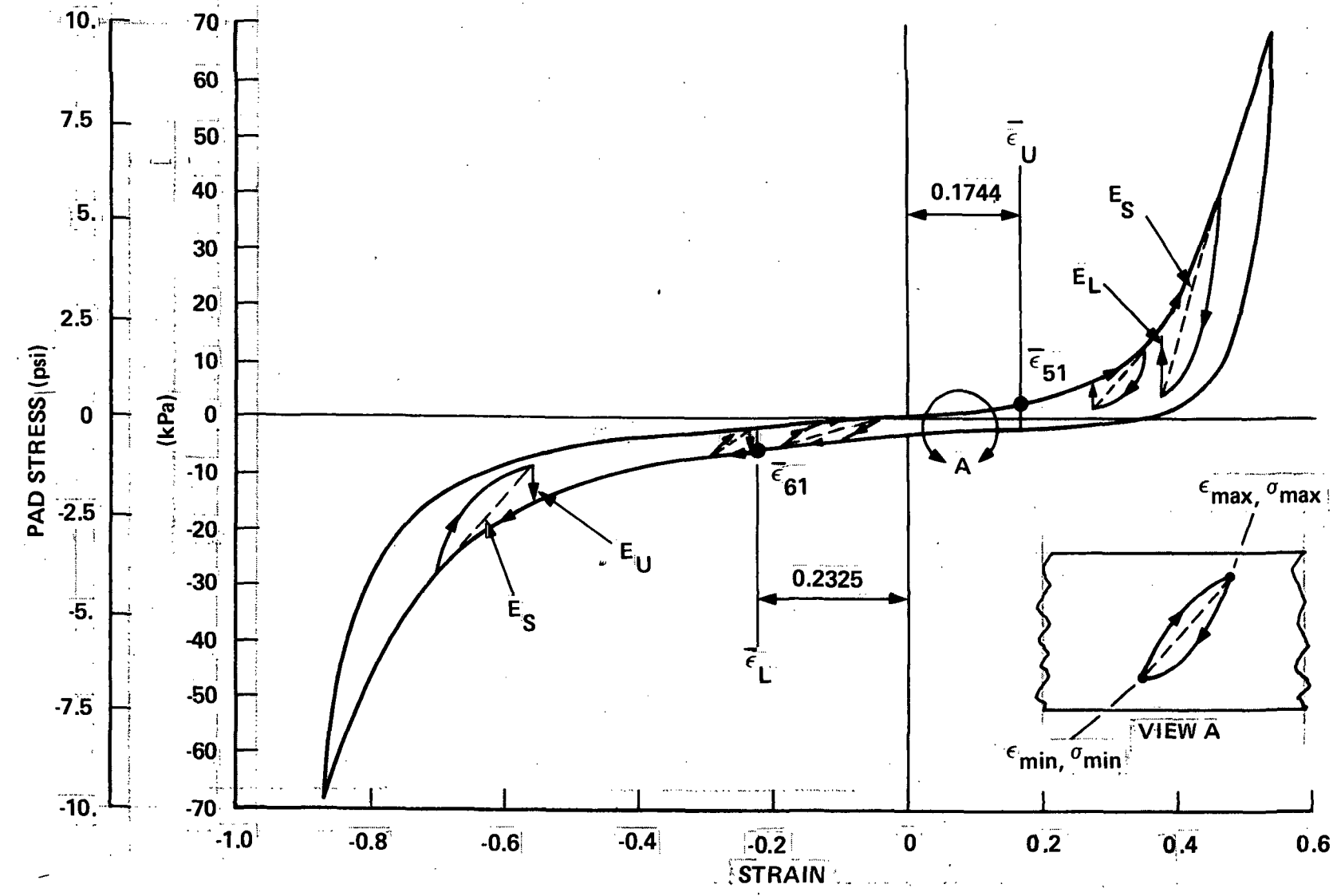


Figure 2. Loading/Unloading Paths Within A Conditioned Hysteretic Envelope  
 [Pad Thickness = 0.406 cm (0.160 in.)].

21

## PAD RESPONSE TENSILE STRESS LEVELS

### Oscillating Tile Pressure in the Presence of a Steady Tile Pressure

The response of a square LI 900 tile was studied with sinusoidal oscillating differential tile pressure,  $p_2$ , in the range of 1.72 kPa (.25 psi) to 13.8 kPa (2.0 psi) at frequencies up to 400 Hertz in the presence of four different steady (nonoscillatory) pressure levels,  $p_1$ , equal to 0.0, -6.89, -13.8, and +6.89 kPa (0.0, -1.0, -2.0 and +1.0 psi). (Positive pressures are in the negative direction denoted as inboard.) The variation of pad tensile stress with frequency of applied sinusoidal pressure, in the absence of steady pressure, ( $p_1 = 0$ ) is presented in Figure 3. The frequency at which the maximum pad tensile stress occurs is defined as the resonant frequency. The resonant frequency has a minimum value of 80 Hertz when the oscillating pressure amplitude is in the range of 5.17 to 8.62 kPa (.75 to 1.25 psi). This is similar to the values found in reference 3. From this plot it is evident that the range of highest tensile stress in the pad will occur when the oscillating pressure is in the range of 60 to 120 Hertz.

When the steady pressure is -6.89 kPa (-1.0 psi) outboard, multiple peak pad stresses occur as shown in Figure 4. Each peak is associated with a different amount of lead or lag of the input loading frequency with respect to the tile response frequency. This multiple peak phenomenon is discussed in the next section. The -6.89 kPa (-1.0 psi) steady outboard pressure on the tile is equivalent to 9.93 kPa (1.44 psi) stress in the pad because of the tile-area/pad-area ratio. At the lower oscillating pressure amplitude, the resonant frequency is 250 Hertz and decreases to 100 Hertz at the higher amplitudes. When compared with Figure 3, the maximum pad response stress increases by 11.0 to 20.0 kPa (1.6 to 2.9 psi) when the equivalent applied outboard steady pad stress increases only 9.93 kPa (1.44 psi). When the steady tile outboard pressure is increased to -13.8 kPa (-2.00 psi) the resonant frequencies increase further, but the pad peak stress response decreases as shown in Figure 5. At low amplitude of oscillating pressure the resonant frequency is 210 to 220 Hertz. There is a

discontinuous shift to a higher frequency of 310 Hertz when  $p_2$  is increased to 5.17 kPa (.75 psi). When the value of  $p_2$  is further increased to 13.8 kPa (2.00 psi) the resonant frequency discontinuously shifts to the lower multiple peak of 160 Hertz.

When the steady tile pressure of 6.89 kPa (1.0 psi) was applied in the inboard direction, the resonant frequency decreases to 50 Hertz at the higher oscillating pressure amplitudes as shown in Figure 6. When compared with the condition of zero steady pressure of Figure 3, the pad stress response is considerably suppressed and the resonant frequencies are lower when this steady 6.89 kPa (1.0 psi) inboard pressure is applied.

Figures 3, 4, 5 and 6 can be used to find the pad stress for a LI 900 tile subjected to a specific combination of oscillating tile pressure and steady tile pressure. For different mass tiles, the pad stress can be adjusted by using the multiplying factors discussed later.

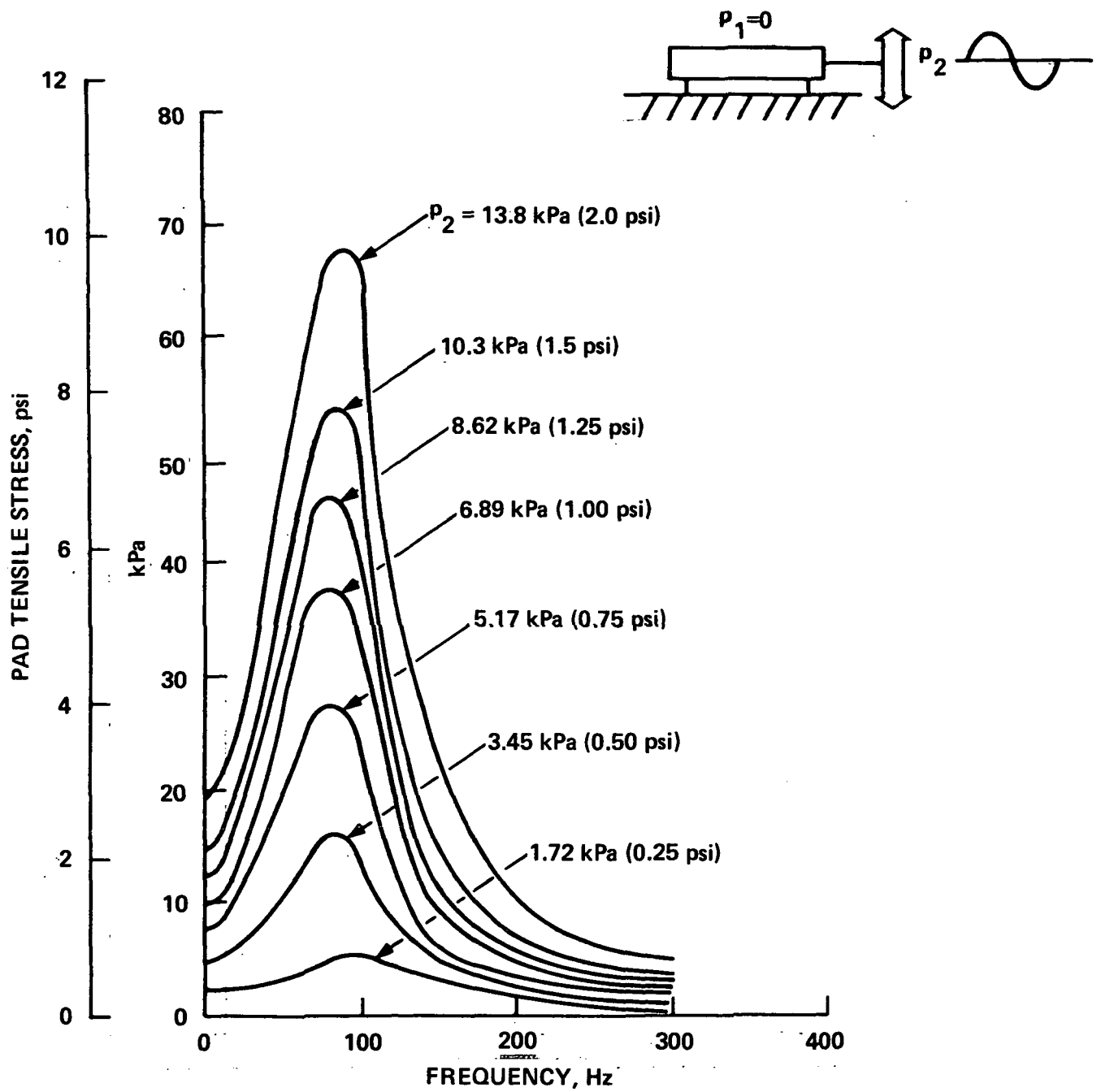


Figure 3. Variation of Pad Tensile Stress With Frequency of Applied Sinusoidal Pressure in Absence of Steady Pressure.

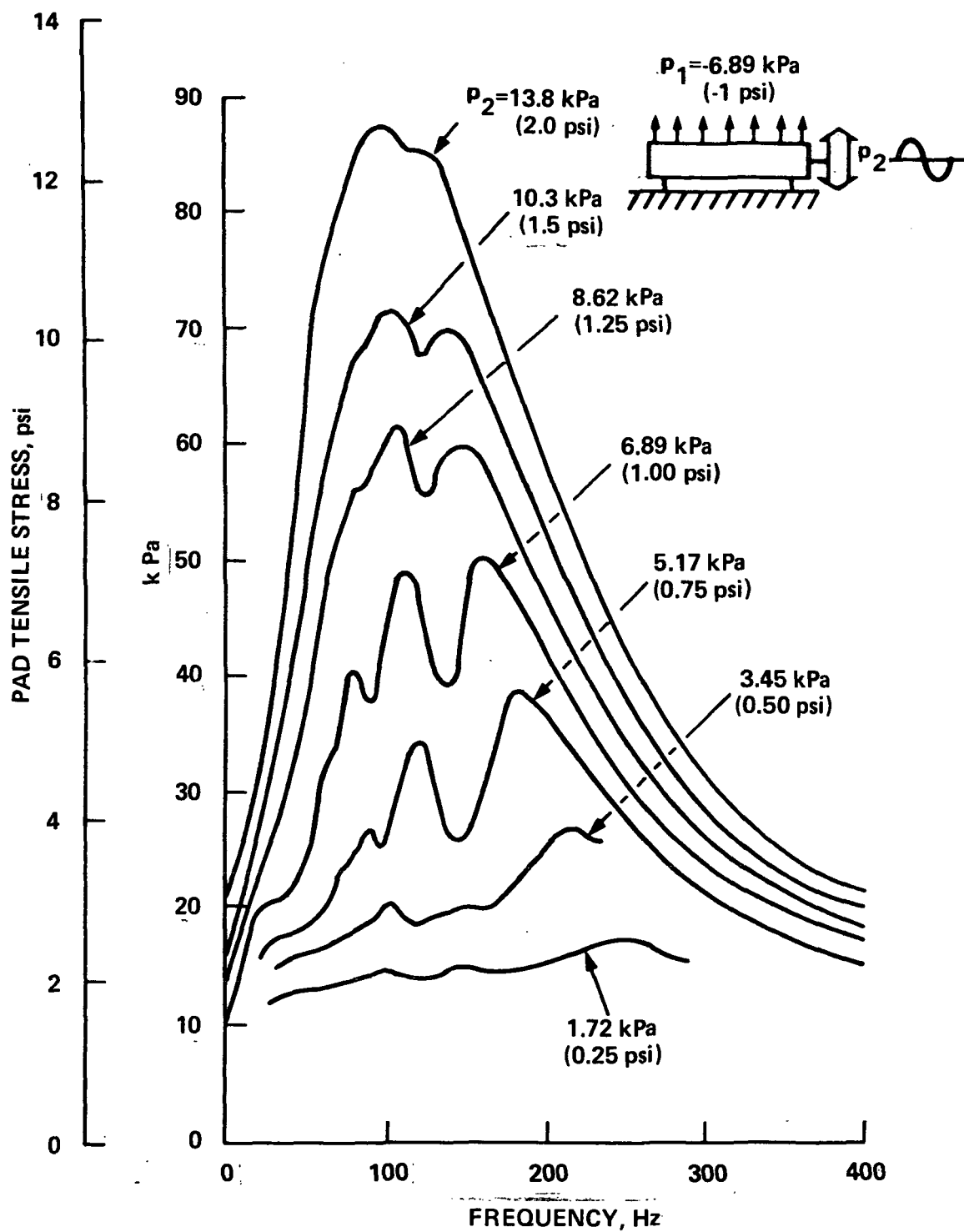


Figure 4. Variation of Pad Tensile Stress With Frequency of Applied Sinusoidal Pressure in the Presence of a Steady Outboard Pressure of  $-6.89 \text{ kPa}$  (-1 psi).

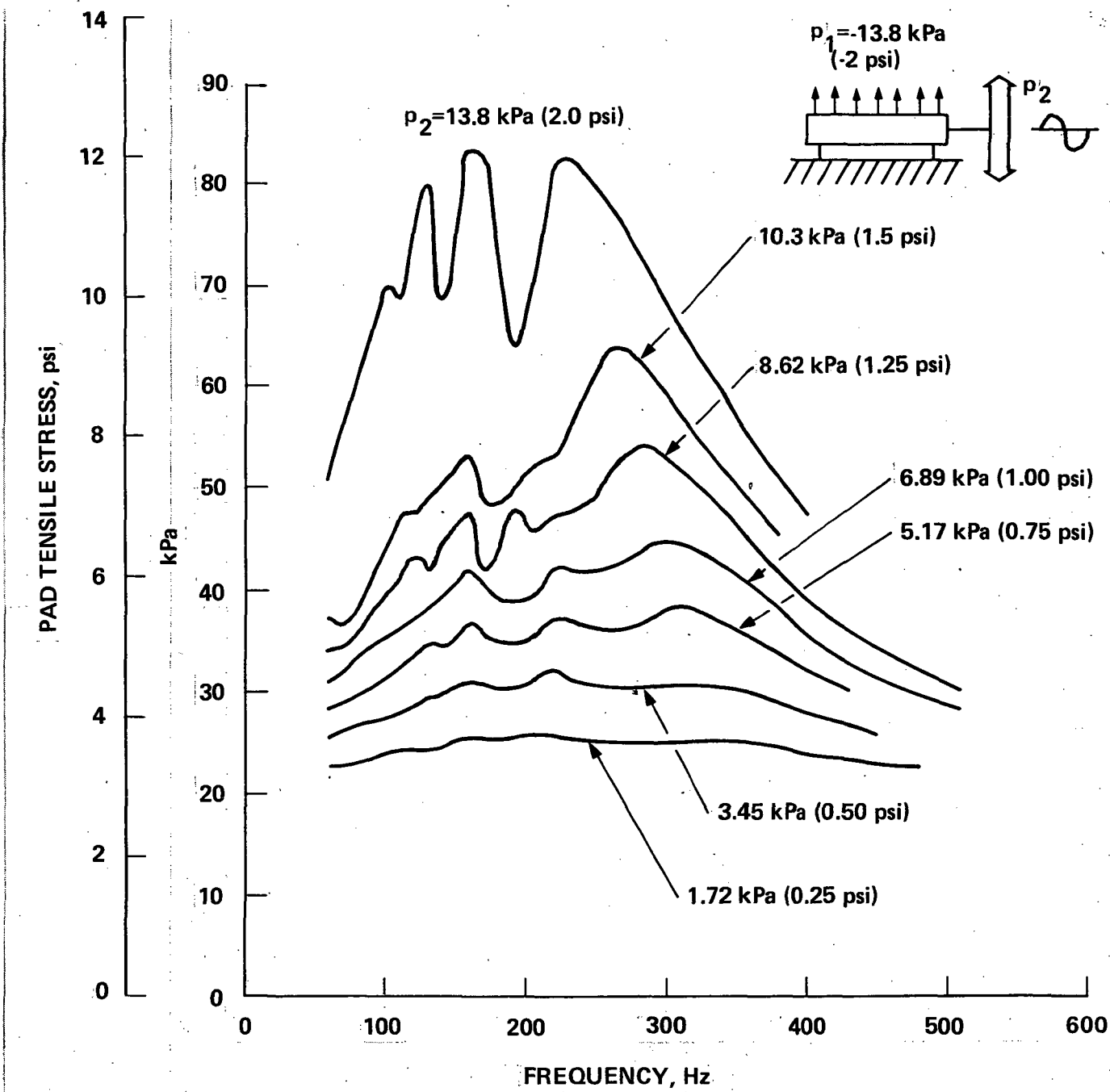


Figure 5. Variation of Pad Tensile Stress With Frequency of Applied Sinusoidal Pressure in the Presence of a Steady Outboard Pressure of  $-13.8 \text{ kPa}$  ( $-2 \text{ psi}$ ).

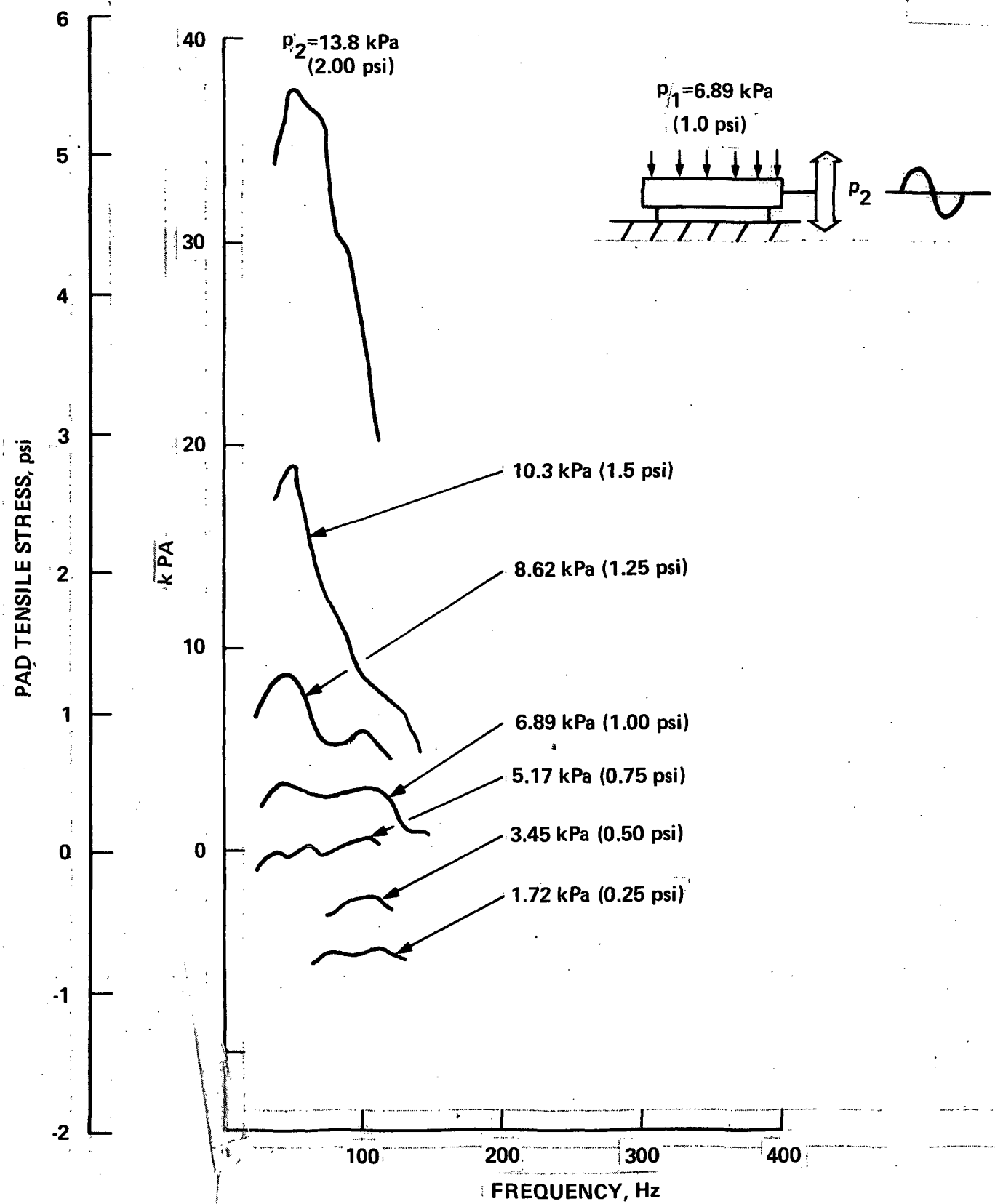


Figure 6. Variation of Pad Tensile Stress With Frequency of Applied Sinusoidal Pressure in the Presence of a Steady Inboard Pressure of 6.89 kPa (1 psi).

### Multiple Peak Resonant Frequencies

As previously mentioned, the resonant frequency of the system for a fixed excitation level has been defined herein as that frequency at which the peak pad tensile stress occurs. When the tile is oscillating in the absence of a steady state load, the variation of pad stress with frequency reveals only one peak and hence one resonant frequency as shown, for example, in Figure 3. However, as a consequence of the highly nonlinear pad behavior, when a steady inboard or outboard load is applied, multiple peaks may appear as shown in Figures 4, 5 and 6 and the selection of a resonant frequency becomes ambiguous. For example, Figure 4 reveals three multiple peaks for the case of an oscillating pressure of 5.17 kPa (.75 psi) and steady outboard pressure of -6.89 kPa (-1.00 psi) occurring at 90, 120 and 180 Hertz. In all three cases the response frequency was the same as the excitation frequency. It was observed that in the region of each peak frequency there was a unique stress-strain loop and stress time trace as shown in Figures 7, 8 and 9. At frequencies above 150 Hertz, in the region of the 180 Hertz peak pad stress frequency, the stress-strain loops were similar in shape to that shown in Figure 7 with a continuous unloading curve. The largest response pad stress in this region was 38.6 kPa (5.6 psi) at the 180 Hertz frequency where the excitation frequency was leading the response frequency by 65 degrees. From 100 to 150 Hertz the stress strain loops were of the form shown in Figure 8 with a discontinuous unloading curve and two peak pad stresses per cycle. In the center of this region, at 120 Hertz, the secondary peak response pad stress of 33.8 kPa (4.9 psi) occurred. In this frequency region, the excitation and response were nearly in phase. Below 100 Hertz, there was a third frequency region where the stress-strain loops were of the form shown in Figure 9. This stress-strain loop also has a discontinuous unloading curve but of a different shape when compared with the shape in Figure 8. Near the upper end of this frequency range, at 90 Hertz, another secondary peak response pad stress of 26.2 kPa (3.8 psi) occurred and the excitation frequency lagged the response frequency by 13 degrees.

*Termed*

Though there are three response peaks, nevertheless the phase difference between the response and the excitation only underwent one  $180^{\circ}$  shift when measured from a frequency just below the first peak to one just above the third peak. Hence it appears that only one resonant condition is actually indicated by the presence of multiple peaks. Consistent with the definition used herein the resonant frequency displayed on succeeding figures is that associated with the highest peak, but it must be recognized, that, as a consequence of the preceding discussion, a distinct resonant frequency in this highly nonlinear system is quite elusive. As will be later observed, this definition of resonant frequency can, in the presence of multiple peaks, lead to discontinuities in curves displaying the variation of resonant frequency with amplitude of excitation since different peaks may dominate the response at different amplitudes.

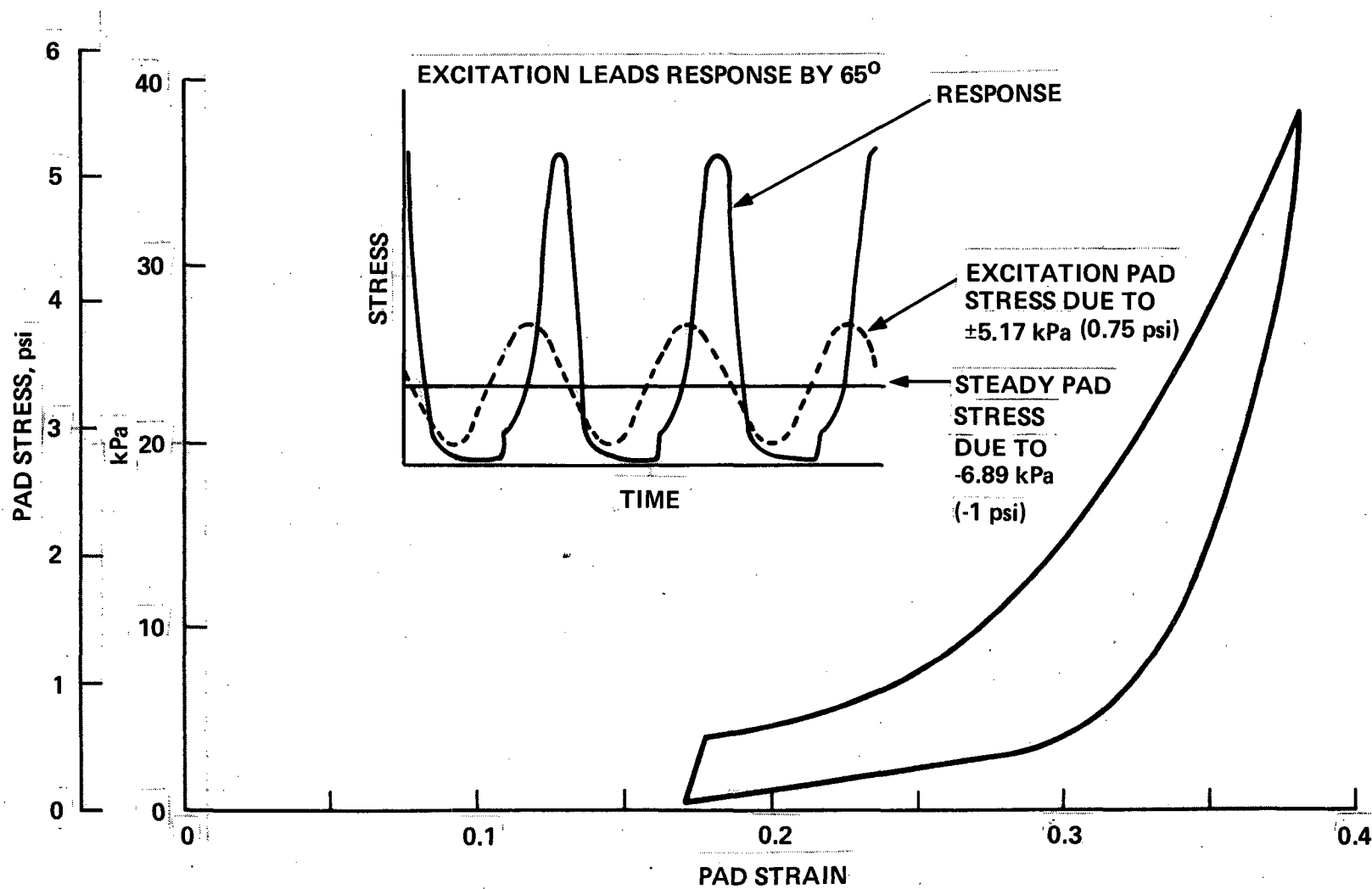


Figure 7. Variation of Pad Stress with Strain and With Time During a Cycle for Steady Outboard Pressure in the Presence of an Oscillating Pressure at 180 Hz.

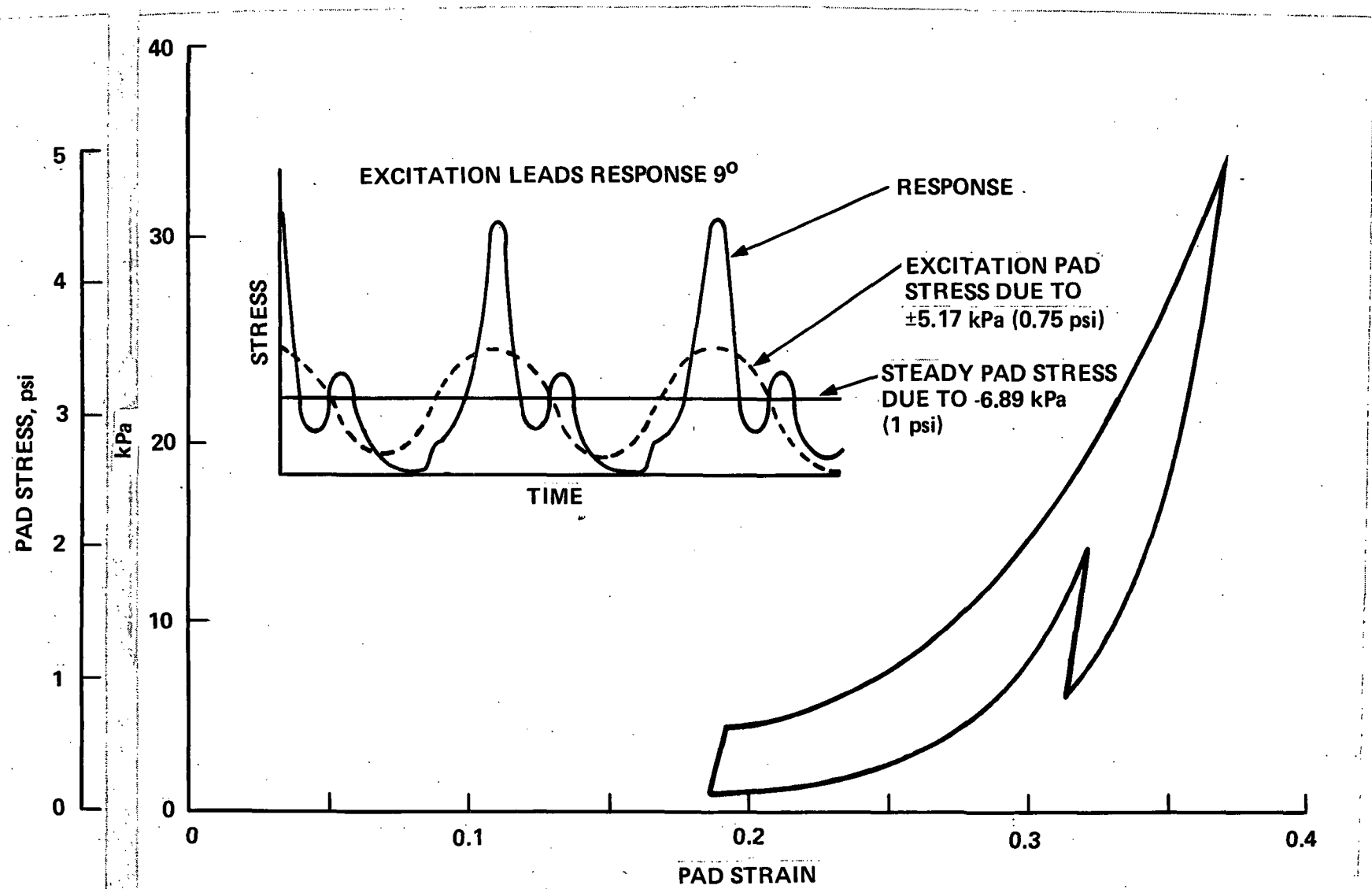


Figure 8. Variation of Pad Stress with Strain and With Time During a Cycle for Steady Outboard Pressure in the Presence of an Oscillating Pressure at 120 Hz.

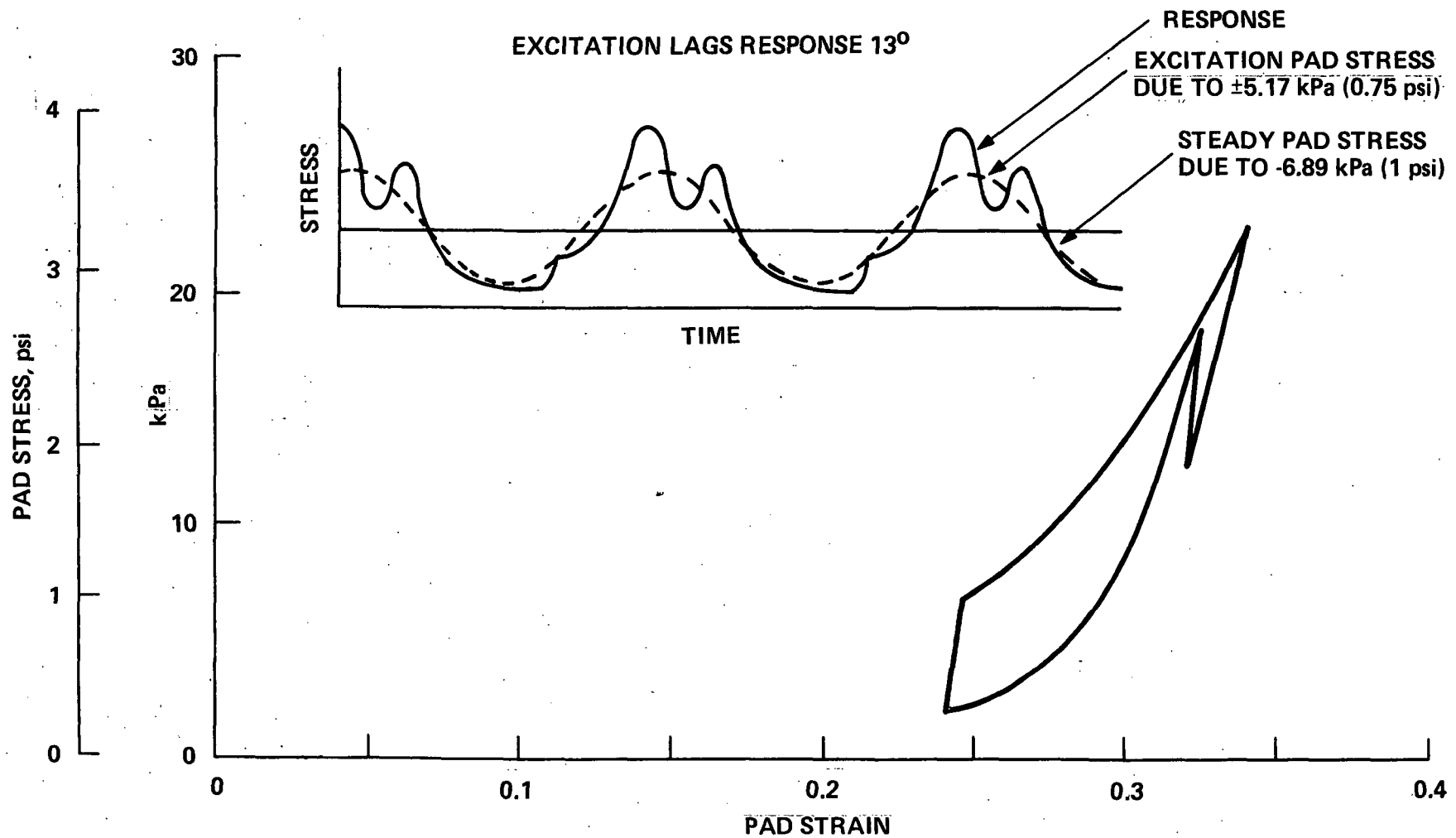


Figure 9. Variation of Pad Stress With Strain and With Time During a Cycle for Steady Outboard Pressure in the Presence of an Oscillating Pressure at 90 Hz.

## Oscillating Substrate in the Presence of a Steady Tile Pressure

The parametric evaluation of an oscillating substrate was performed for the square LI 900 tile on a .437 cm (.172 in) pad shown in Figure 1. The sinusoidal substrate vibration acceleration amplitude,  $\alpha$ , was varied from 5 to 140 at frequencies up to 400 Hz. Four different steady pressure levels,  $p_1$ , equal to 0.0, -6.89, -13.8, and + 6.89 kPa (0.0, -1.0, -2.0 and + 1.0 psi) were used. The variation of pad tensile stress with applied sinusoidal frequency when the tile steady pressure is zero, is presented in Figure 10. Here the minimum resonant frequency is 80, identical to the case for oscillating tile pressure in Figure 3.

By comparing the response stresses for the substrate oscillations in Figure 10 with the response stress for the oscillating tile pressure in Figure 3, it is apparent that identical response is obtained. This is to be expected for a steady state condition that results from these two sinusoidal sources of excitation. It can be shown that the response is identical to that obtained by exciting the substrate with an acceleration amplitude given by

$$\alpha_T = \frac{p_2 A_t}{m G} , \quad (4)$$

When an outboard steady pressure of -6.89 kPa (-1.0 psi) is applied to the tile combined with the substrate oscillations, the pad stress response with multiple peaks occur as shown in Figure 11. By comparing this figure with Figure 4 for the oscillating tile pressure, again the shape of the curves are similar. The characteristics of the multiple peaks, each with a different amount of lead or lag of the input loading frequency with respect to the response frequency, was discussed in the previous section. See Figures 7, 8, and 9 for the stress-strain loops and stress time plots of 3 stress peaks. When comparing Figure 11 with Figure 10, it is evident that the pad response stress is increasing at a higher rate than the steady outboard pressure of -6.89 kPa (-1.0 psi) being applied. When the steady tile pressure is increased to -13.8 kPa (-2.00 psi),

the response pad stresses decrease as can be seen in Figure 12. The shape of this curve is similar to Figure 5 for applied pressure oscillations. When an inboard steady tile pressure of 6.89 kPa (1.0 psi) is applied, the resonant frequencies and the pad stress levels decrease as shown in Figure 13. This figure has the same shape as Figure 6 for the tile oscillation case.

Figures 10, 11, 12, and 13 can be used to find the pad stress for a LI 900 tile subjected to a specific sinusoidal substrate acceleration combined with a steady tile pressure. For different mass tiles, the pad stress can be adjusted by using the multiplying factors discussed later.

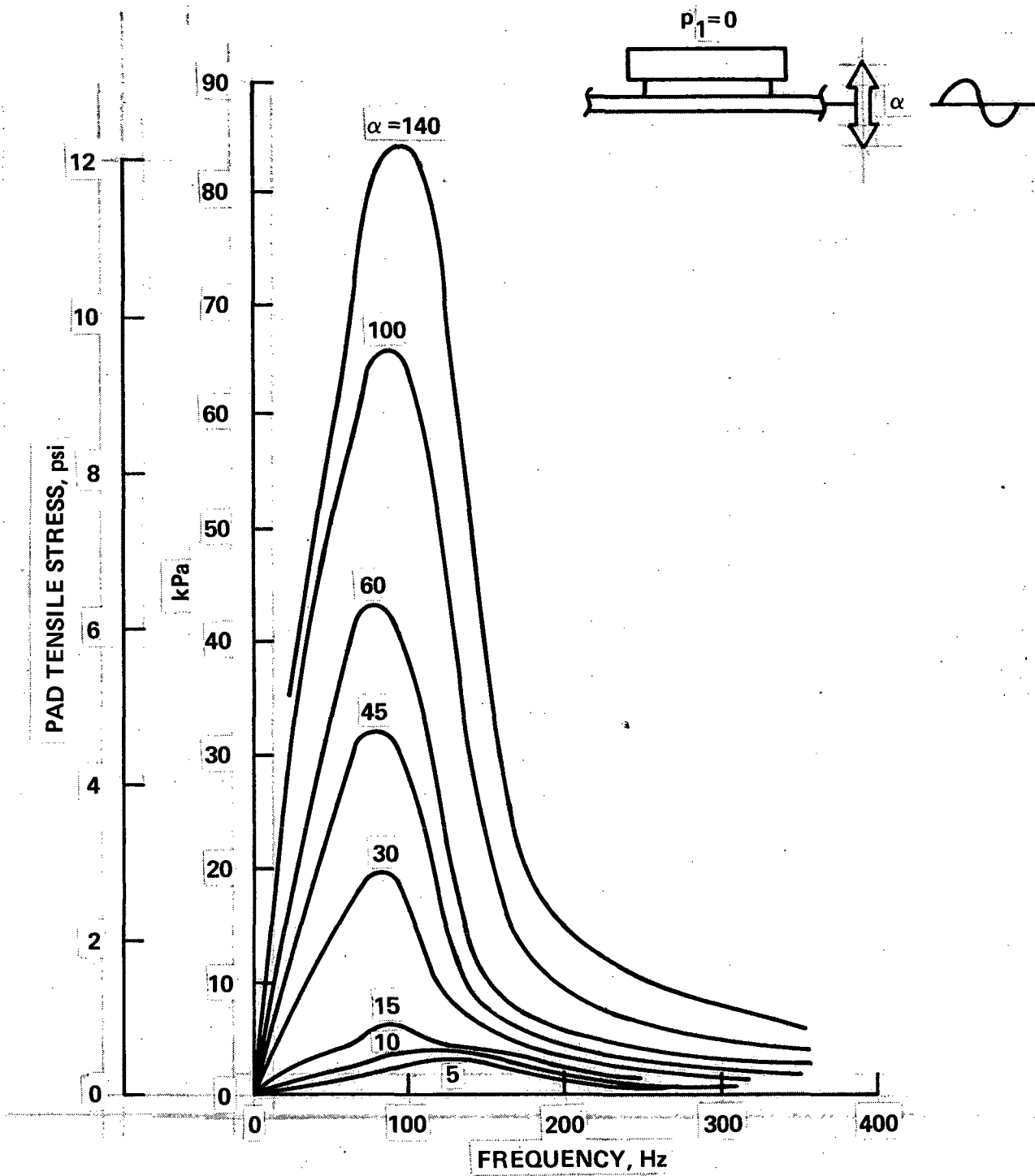


Figure 10. Variation of Pad Tensile Stress With Applied Sinusoidal Substrate Frequency in the Absence of Steady Pressure.

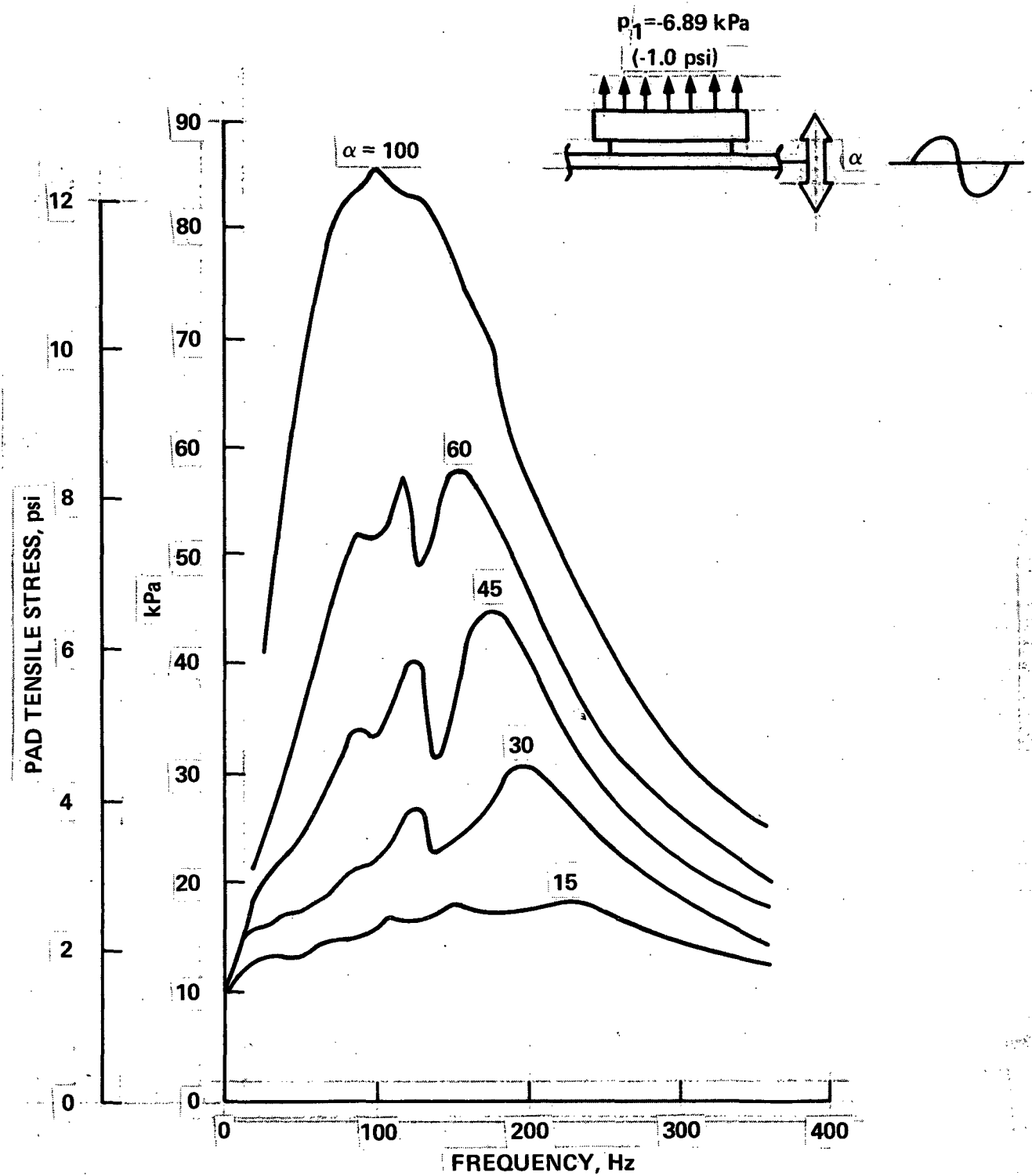


Figure 11. Variation of Pad Tensile Stress With Applied Sinusoidal Substrate Frequency for a Steady Outboard Tile Pressure of  $-6.89 \text{ kPa}$  (-1 psi).

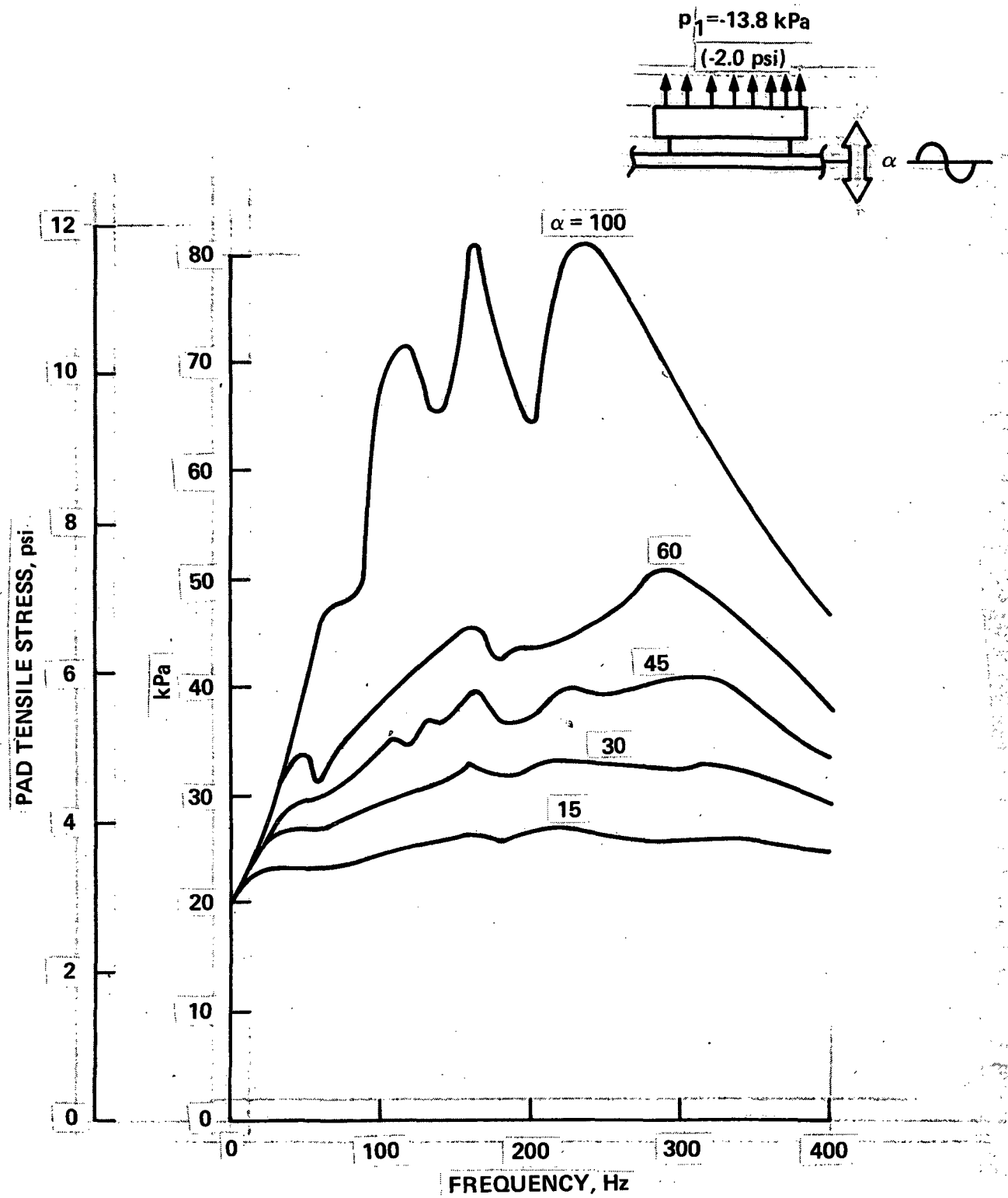


Figure 12. Variation of Pad Tensile Stress With Applied Sinusoidal Substrate Frequency for a Steady Outboard Tile Pressure of -13.8 kPa (-2 psi).

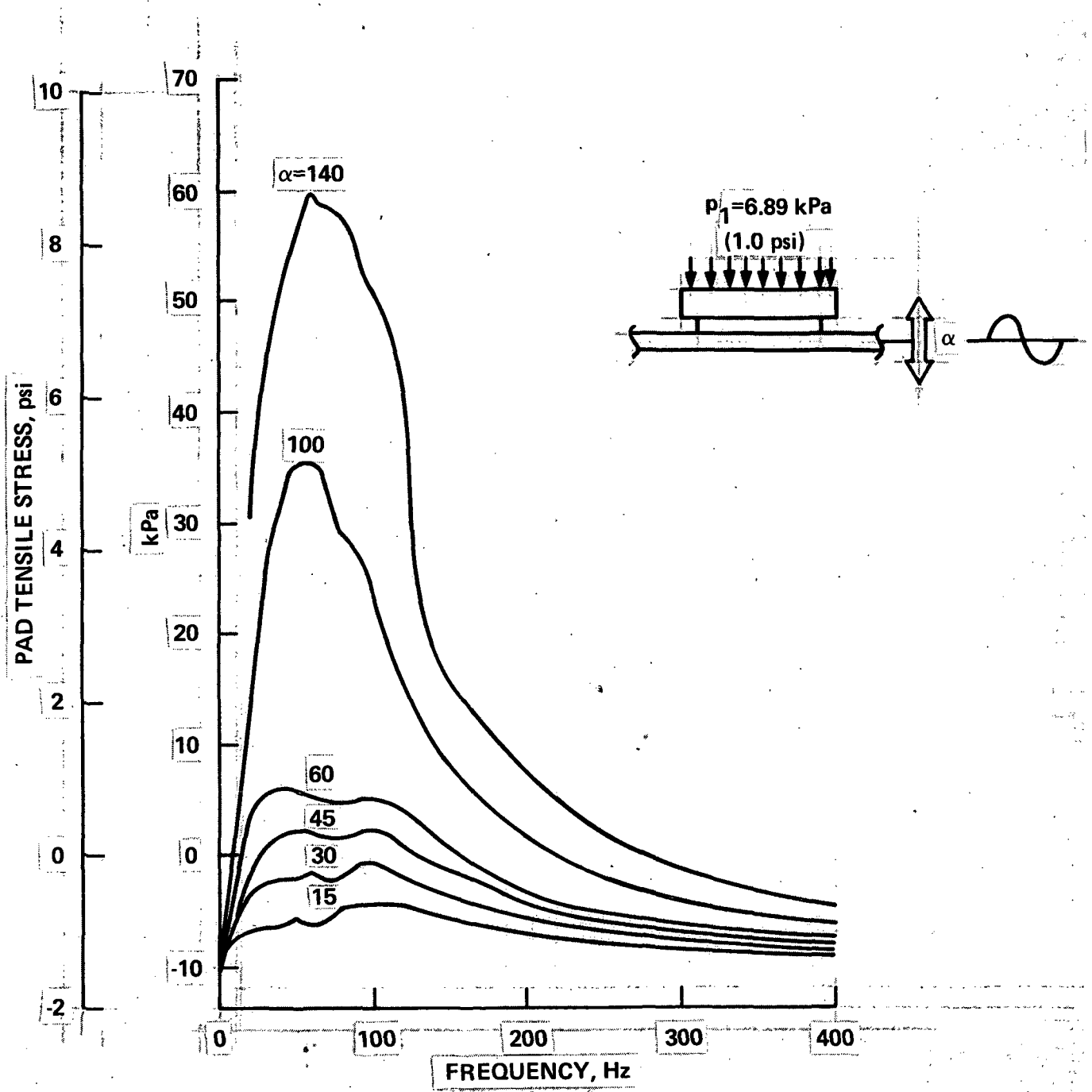


Figure 13. Variation of Pad Tensile Stress With Applied Sinusoidal Substrate Frequency for a Steady Inboard Tile Pressure of 6.89 kPa (1 psi).

## VARIATION OF NONLINEAR RESPONSE WITH EXCITATION AMPLITUDE

This section presents the variation of the maximum pad stress, the resonant frequency, and the magnification factor with excitation amplitude.

### Pad Maximum Stress

The magnitude of the pad maximum stress as a function of the tile sinusoidal pressure level,  $P_2$ , or the substrate acceleration amplitude,  $\alpha$ , is presented in Figure 14 for variations in the steady tile pressure from 6.89 kPa (1.0 psi) inboard to -13.8 kPa (-2 psi) outboard. For a linear system all of the curves of Figure 14 would be parallel straight lines with the spacing between them being the difference in the steady pressure. However, these nonlinear stress curves deviate considerably from this pattern. One important observation is that by applying a steady differential pressure inboard, the maximum pad stress is decreased considerably. If the oscillating pressure is 6.89 kPa (1.0 psi), the addition of 3.45 kPa (0.5 psi) steady pressure inboard reduces the pad stress from 37.2 kPa (5.4 psi) to 17.9 kPa (2.6 psi), or a change of -19.3 kPa (-2.8 psi). The amount of pad stress suppression is 5.6 times the steady inboard tile pressure being applied. Repeating this process for a change in the steady inboard pressure of 6.89 kPa (1.0 psi), the rate is 5.0 times the applied inboard pressure. This is a significant reduction and indicates that if there is a steady inboard pressure on the tile at the time of maximum tile or substrate oscillations, there will be a significant reduction in pad stresses. Conversely, a steady outboard pressure of -6.89 kPa (-1.0 psi) will have a slightly aggravating effect, but the rate is smaller than 2 times the applied outboard pressure. As the steady tile outboard pressure increases above -6.89 kPa (-1.0 psi) to -13.8 kPa (-2.0 psi), the maximum pad stress decreases when the sinusoidal pressure is above 5.17 kPa (0.75 psi) or the substrate acceleration amplitude is above 40.

If the maximum pad stress is desired for a LI 900 tile at resonant frequency for a specific substrate acceleration amplitude or a tile sinusoidal pressure amplitude combined with a steady tile pressure, Figure 14 may be used. Changes in stress with changes in mass can be made by using the stress multiplying factor discussed later.

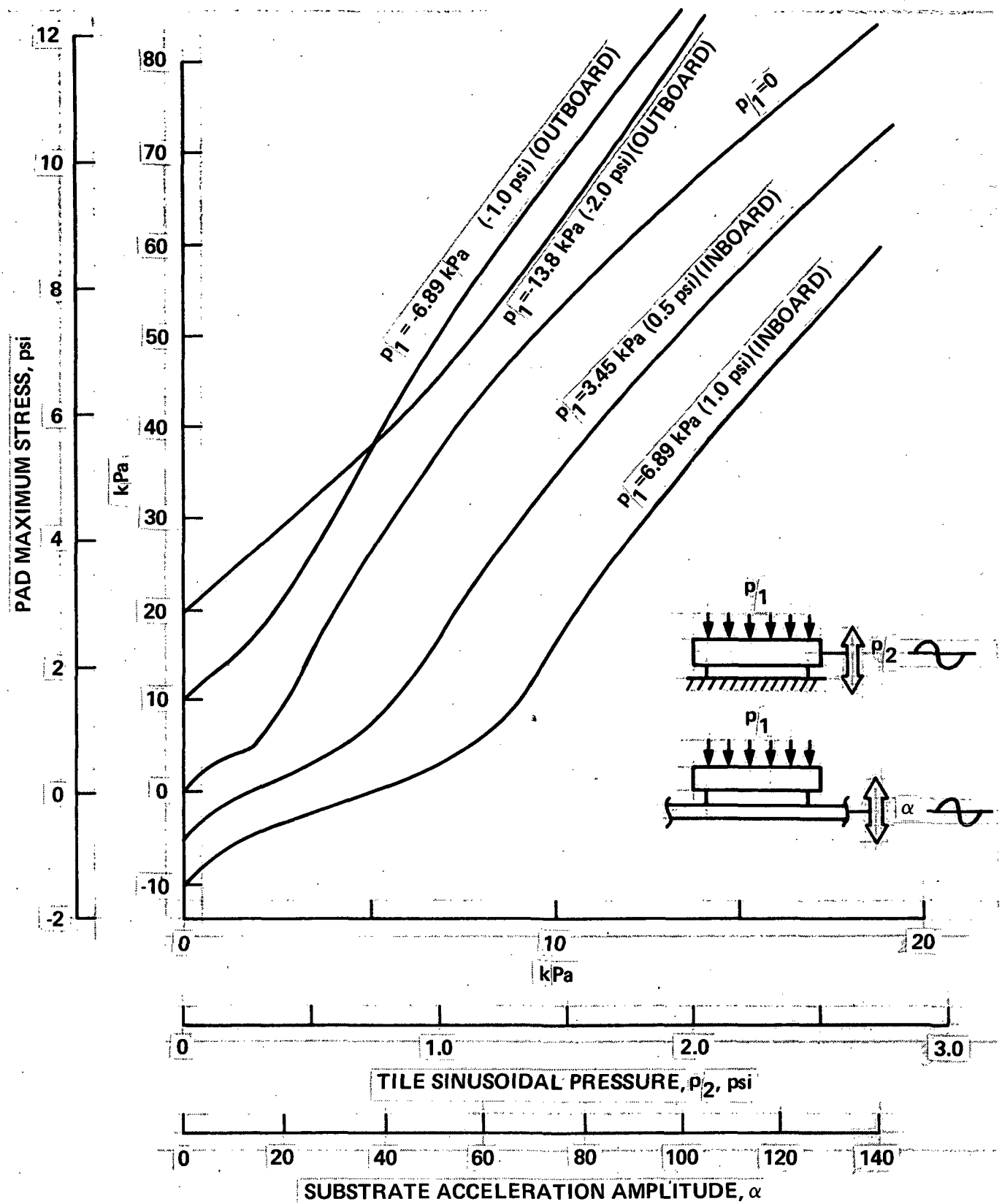


Figure 14. Variation of Pad Maximum Stress With Input Amplitude.

### Tile Resonant Frequency

Figure 15 presents the variation of the tile resonant frequency with applied sinusoidal pressure amplitude or with substrate acceleration amplitude. With no steady tile pressure present, the shape of the curve is similar to that presented in Reference 3. At low amplitude the resonant frequency decreases with increasing amplitude to a minimum value of 80 Hz, and slowly increases with increasing input amplitude. Due to the appearance of multiple peak responses as discussed earlier, discontinuities in these curves can occur. As the steady inboard pressure of 6.89 kPa (1.0 psi) is applied, there is a discontinuous jump to a lower resonant frequency as the sinusoidal excitation amplitude increases. When the steady pressure is -6.89 kPa (-1.00 psi) outboard, there is also a discontinuous jump to a lower frequency when the sinusoidal input amplitude is increased. In each case the shift is from a higher to a lower resonant frequency as the pressure input amplitude is increased. The one exception is for  $p_1$  equal to -13.8 kPa (-2.0 psi) at the lower input amplification levels. The most significant observation from Figure 15 is that there is a large increase in resonant frequency when the tile steady pressure is outboard.

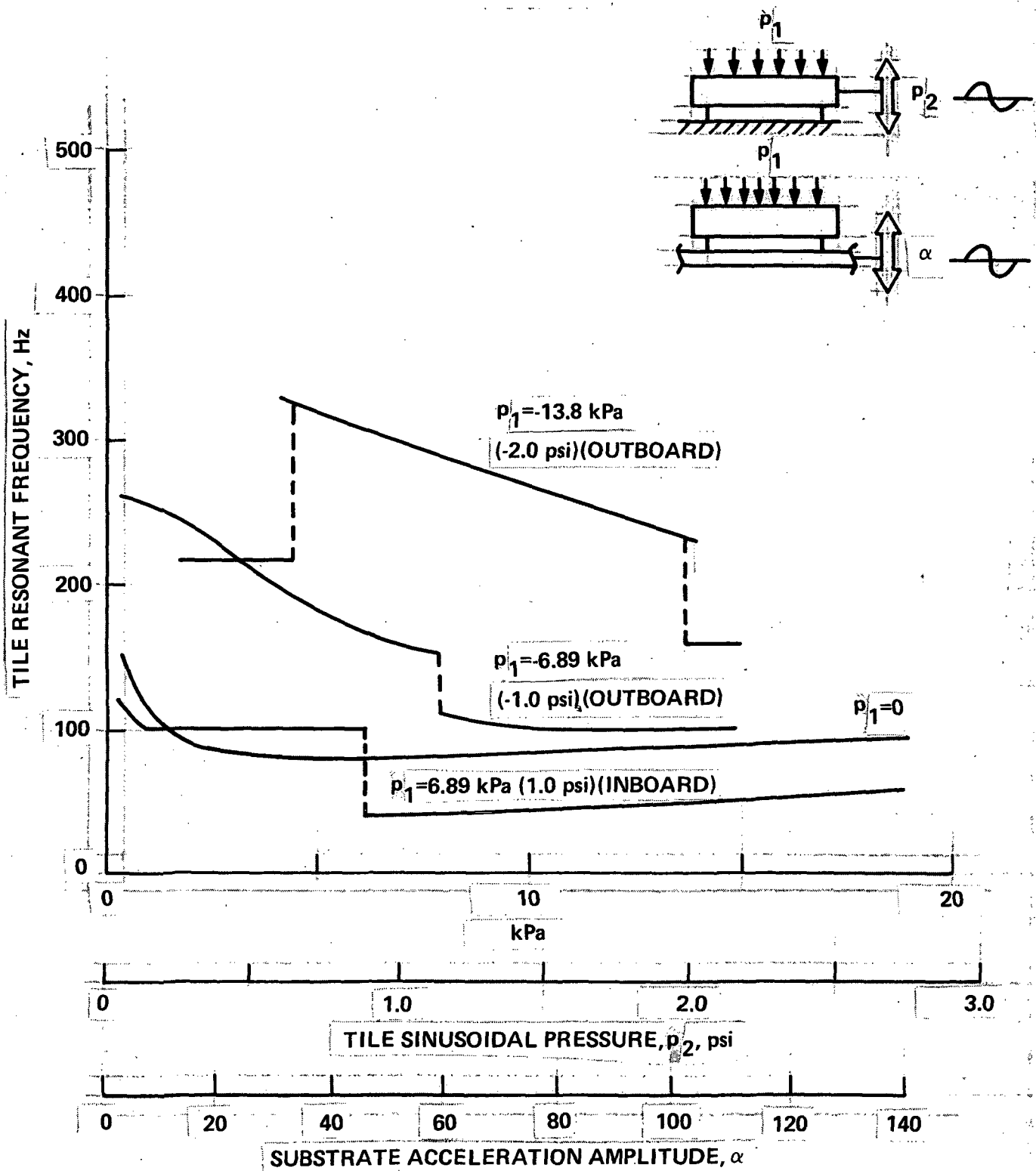


Figure 15. Variation of Tile Resonant Frequency With Input Amplitude.

### Maximum Magnification Factor

Figure 16 presents the maximum magnification factor,  $f_s$ , for the sinusoidal pressure case as

$$f_s = \frac{\sigma + P_1 A_t / A_p}{P_2 A_t / A_p} \quad (5)$$

where

- $\sigma$  is pad maximum response pad stress
- $P_1$  is tile steady pressure (positive inboard)
- $P_2$  is tile sinusoidal pressure
- $A_t$  is tile area
- $A_p$  is pad area

This is the magnification based on the sinusoidal pressure component only. For the substrate oscillating case the magnification factor is

$$f_s = \dot{w} / \alpha G \quad (6)$$

where

- $\dot{w}$  is the tile acceleration
- $\alpha$  is the substrate input acceleration amplification
- $G$  is the acceleration of gravity

Over most of the range the largest magnification occurs for a steady outboard pressure of -6.89 kPa (-1.0 psi) with the maximum value being 4.15. In general the magnification factor increases with increasing outboard steady pressure on the tile up to -6.89 kPa (-1.0 psi), and then decreases as the outboard steady pressure increases above -6.89 kPa (-1.0 psi). The magnification factor is suppressed to values below 2 over most of the range when an inboard steady pressure of 6.89 kPa (1.0 psi) is applied to the tile.

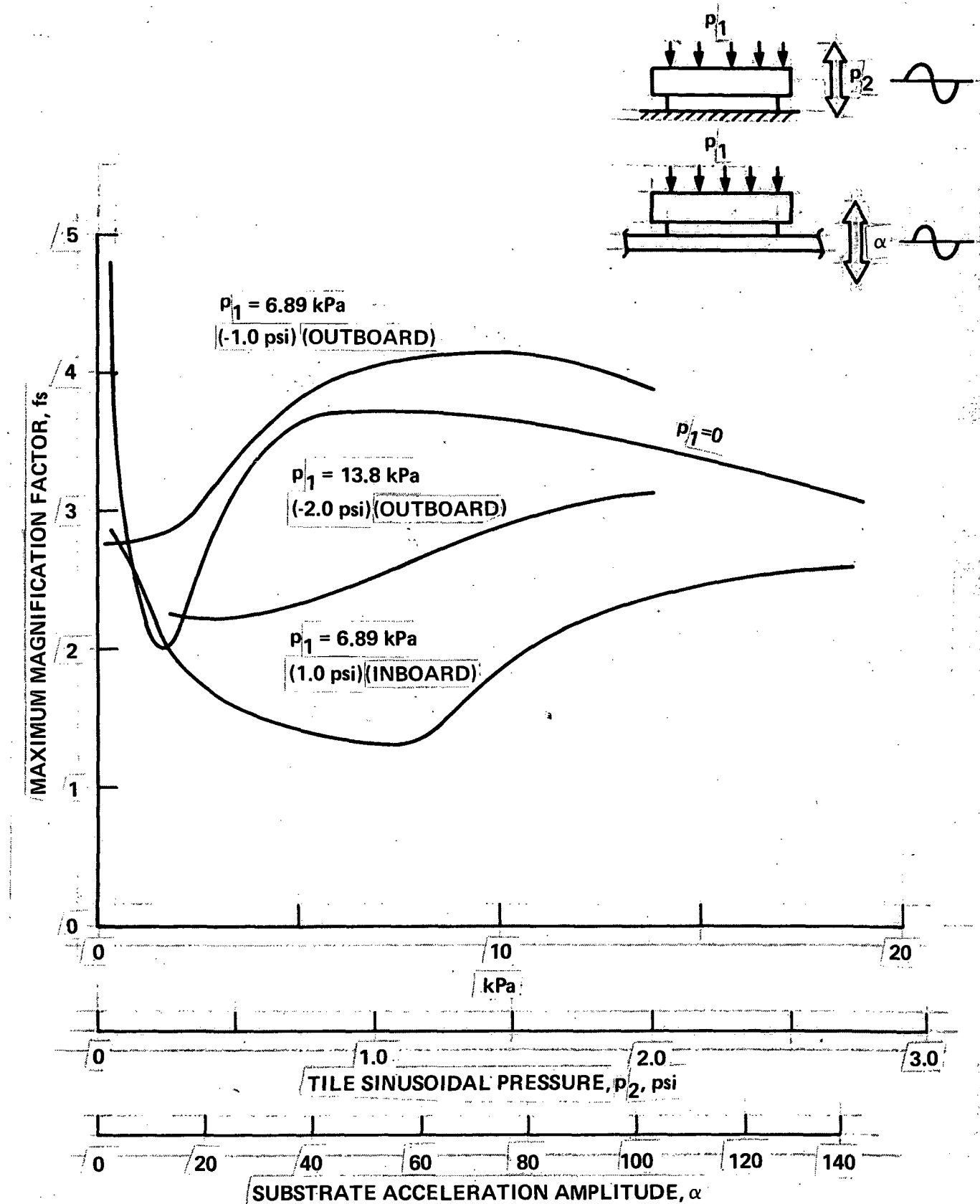


Figure 16. Variation of Maximum Magnification Factor With Input Amplitude.

VARIATION OF NONLINEAR RESPONSE WITH TILE  
STEADY DIFFERENTIAL PRESSURE

The variation of pad maximum response stress and magnification factor in the presence of inboard and outboard steady pressure are shown in Figures 17, 18, 19, and 20. The maximum pad stress occurs when the steady stress is -6.89 kPa (-1.0 psi) outboard (Figures 17 and 18), while the peak magnification factor occurs when the steady pressure is approximately -3.45 kPa (-.5 psi) outboard (Figures 19 and 20). As shown in Figures 17 and 18, the pad stress decreases rapidly when steady inboard pressure is applied. For this tile, the weight of the tile will exert a .193 kPa (0.028 psi) static stress on the pad when the tile is in an upright position at sea level. The slope of the curves at a tile steady pressure of zero in Figures 17 and 18 is such that if the analysis neglected this .193 kPa (0.28 psi) steady stress, the error would be an indicated pad stress that is 2 percent too low. Figures 17 through 20 indicate that the response stress and magnification factor are considerably reduced by imposing a steady inboard tile pressure in conjunction with the oscillating tile pressure or the substrate motion. These figures indicate that the most severe response pad tensile stresses will occur when there is a -6.89 kPa (-1.0 psi) outboard steady tile pressure superimposed on the tile at the time of dynamic excitation.

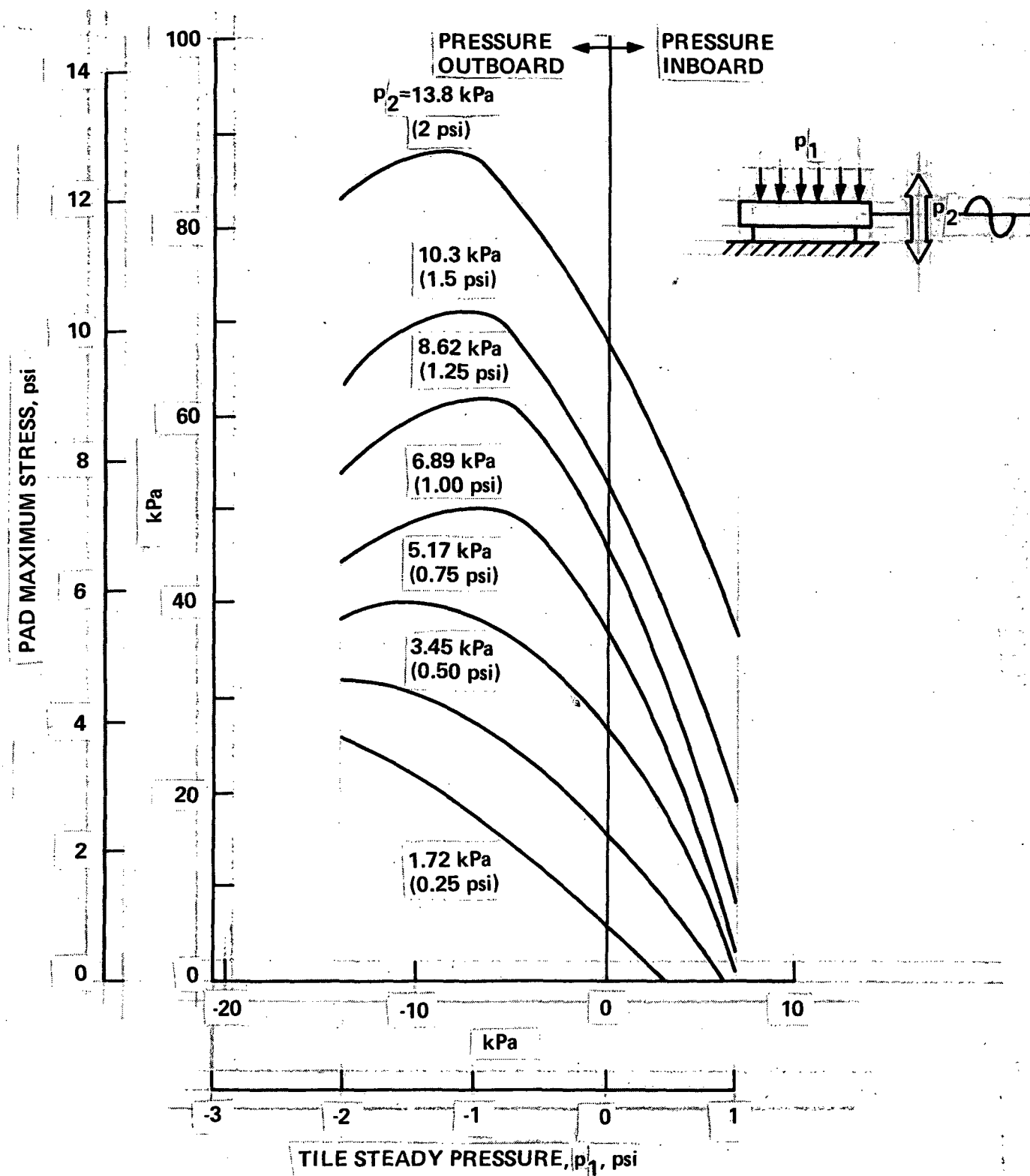


Figure 17. Variation of Pad Maximum Stress With Magnitude of Tile Steady Pressure in the Presence of Oscillating Pressure.

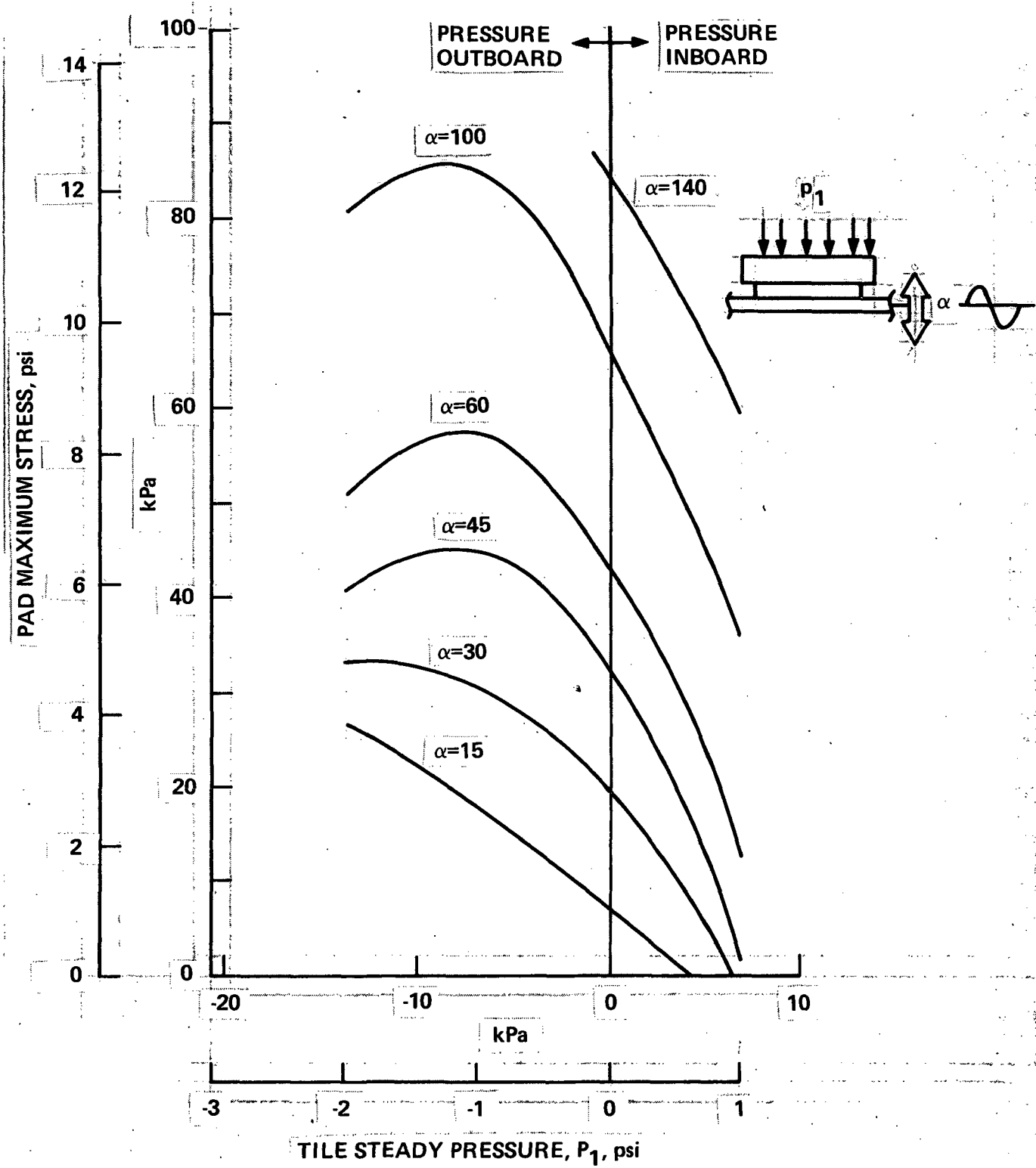


Figure 18. Variation of Pad Maximum Stress With Magnitude of Tile Steady Pressure in the Presence of Substrate Oscillating Acceleration.

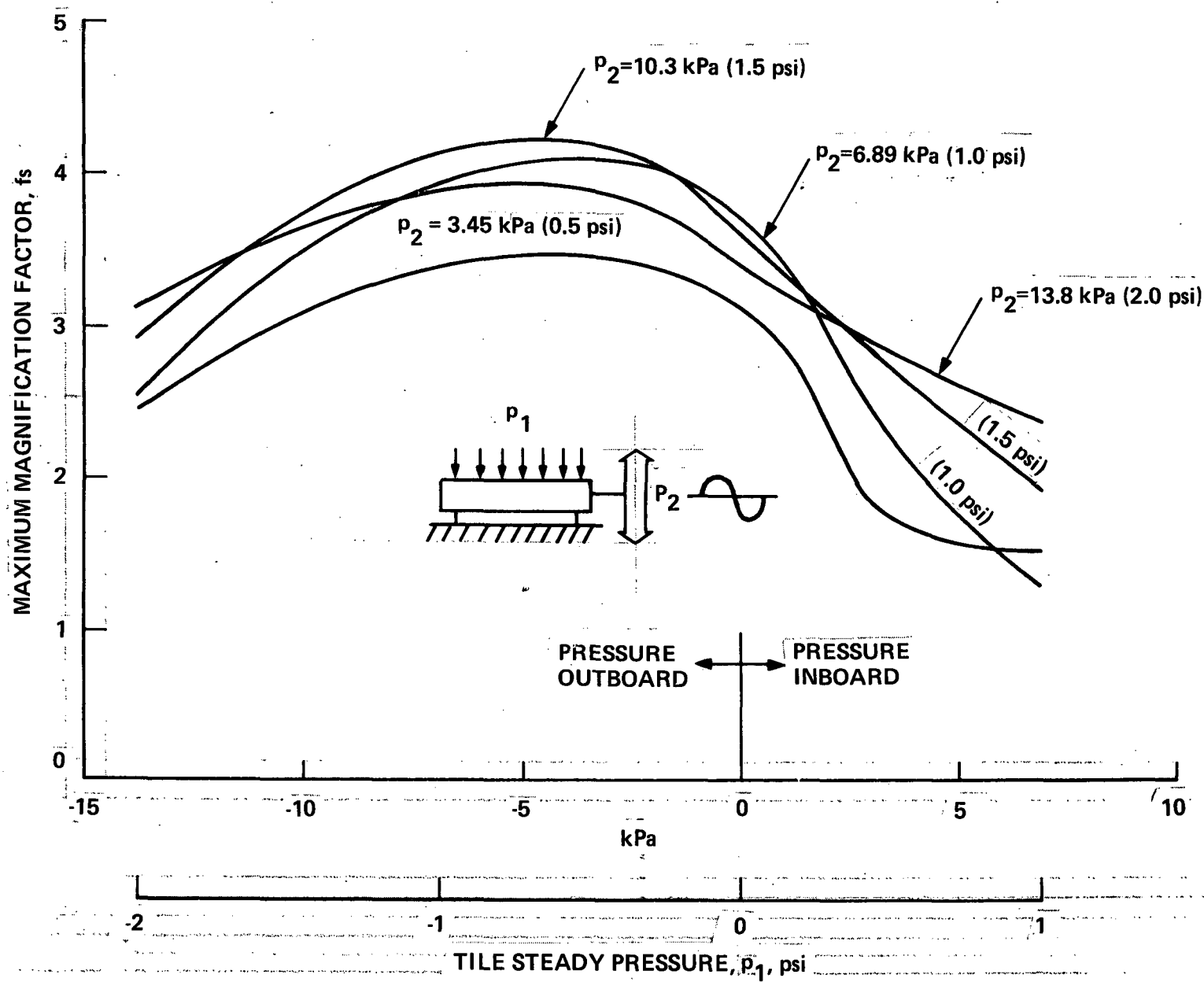


Figure 19. Variation of Maximum Magnification Factor With Magnitude of Tile Steady Pressure in the Presence of Oscillating Pressure.

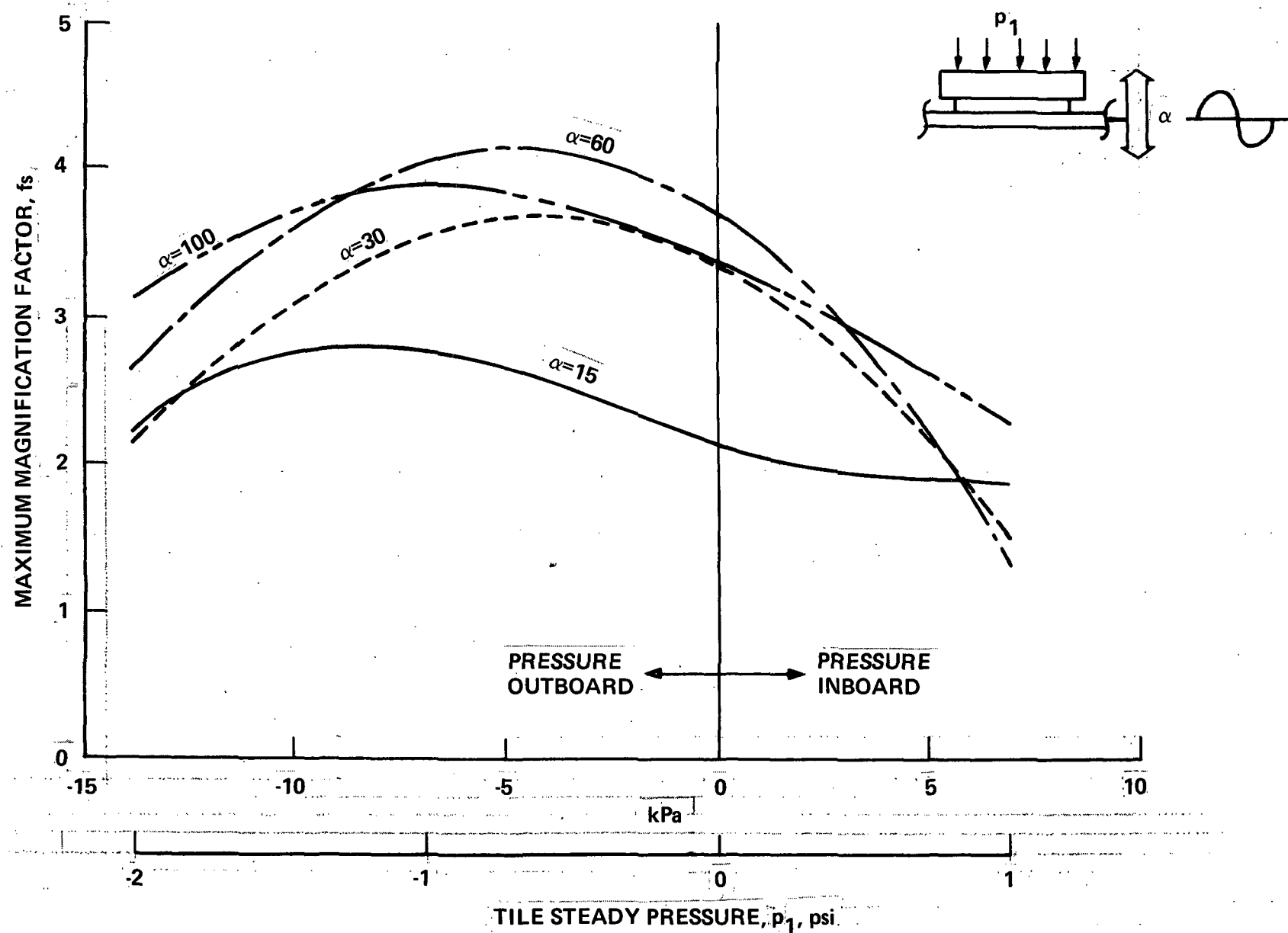


Figure 20. Variation of Maximum Magnification Factor With Magnitude of Tile Steady Pressure in the Presence of Substrate Oscillation.

## NONLINEAR RANDOM RESPONSE AND PAD MATERIAL CONDITIONING EFFECTS

### Comparison of Linear and Nonlinear Predicted Probability of Occurrence for Positive Peak Pad Stresses Due to Random Gaussian Substrate Acceleration

Presently, the predicted pad stress due to random substrate accelerations is based on two assumptions: that the pad behaves in a linear fashion and that the random substrate acceleration driving the tile is Gaussian. In a linear analysis the expected substrate accelerations in the form of power spectral densities (PSD's) may be used along with a linear transform function for a base driven spring/mass/damper system to produce the tile PSD's, tile rms acceleration, rms pad stress and 3-SIGMA pad stress values.

In performing life assessment studies of the thermal protection system it is desirable to assume that the probability of occurrence for positive pad stress peaks follows a Rayleigh distribution. The rms pad stress completely characterizes the assumed Rayleigh distribution and the probability of occurrence for positive pad stress peaks exceeding three times the rms pad stress or 3-SIGMA value is about 3.3%. Therefore, the purpose of this section is to address the validity of the Rayleigh distribution using the nonlinear analysis.

In the nonlinear analysis it is first necessary to generate random Gaussian substrate acceleration histories which have the proper PSD's. These substrate acceleration histories are then used as transient excitations in the nonlinear analysis. The predicted nonlinear pad stress history is then calculated and the data reduced (this includes counting and ordering positive peak stresses) to provide the probability density of positive peak pad stresses as shown in Figures 21 through 27. For the purpose of comparison the Rayleigh distribution linear analysis is superimposed in these figures. Each of the figures gives the tile weight, PSD input spectrum used, linear and nonlinear predicted rms tile response and pad stress. A comparison of the nonlinear predicted probability density of positive peak pad stresses with the assumed Rayleigh distribution is provided where the Rayleigh distribution is normalized on the basis of a linear predicted rms stress. The linear analysis assumes 35% of critical damping and a linear stiffness of

1368 N/cm (781 lb/in). The comparisons indicate that, in general, there is little difference between the linear and nonlinear predicted rms stress values. As a consequence, the Rayleigh distribution generally provides a good approximation for the occurrence of pad stresses near the rms stress value which has the greatest probability of occurrence. However, as the pad stresses get higher, the Rayleigh distribution becomes more inaccurate, with a much higher percentage of peaks occurring beyond 3 times the rms stress value. It is these higher stresses which are most damaging to the life of the thermal protection system. They exceed the Rayleigh distribution prediction due to the presence of nonlinearities in the pad behavior which have more influence when higher pad stresses are present. The greater the tile mass or substrate motion, the higher the pad stress and hence the greater the exceedance of the Rayleigh distribution at its tail end. For example, in a lightweight tile of .106 kPa (.234 lbs.), there is little exceedance of the Rayleigh distribution prediction beyond 3 times the linear rms stress value even in the presence of high level substrate motion. However, in a heavy tile of .319 Kg (.703 lbs.), the Rayleigh distribution prediction is exceeded out to about 6 times the linear rms stress value even in the presence of low level substrate motion. For moderate weight tiles the exceedance will depend on the level of substrate motion.

The results indicate that the linearly predicted rms stress value is reasonably accurate, however, due to nonlinearities in the system, the Rayleigh distribution does not provide an adequate probability of occurrence prediction for high stress peaks and thus the use of "3-SIGMA" value may be unconservative especially for the heavier tiles.

TILE WEIGHT = 0.3186 Kg (0.7025 LBS.)  
 PAD AREA =  $161.3 \text{ cm}^2$  (25 IN.<sup>2</sup>)  
 PAD THICKNESS = 0.4064 cm (0.160 IN.)

$1 \text{ g}^2/\text{Hz}$

9db/OCT

-6db/OCT

75Hz

1300Hz

INPUT  
 41.2 g rms

OUTPUT  
 g rms (LINEAR)=15.5  
 g rms (NONLINEAR)=17.1  
 rms STRESS (LINEAR)=3.034 kPa (0.44 psi)  
 rms STRESS (NONLINEAR)=3.309 kPa (0.48 psi)

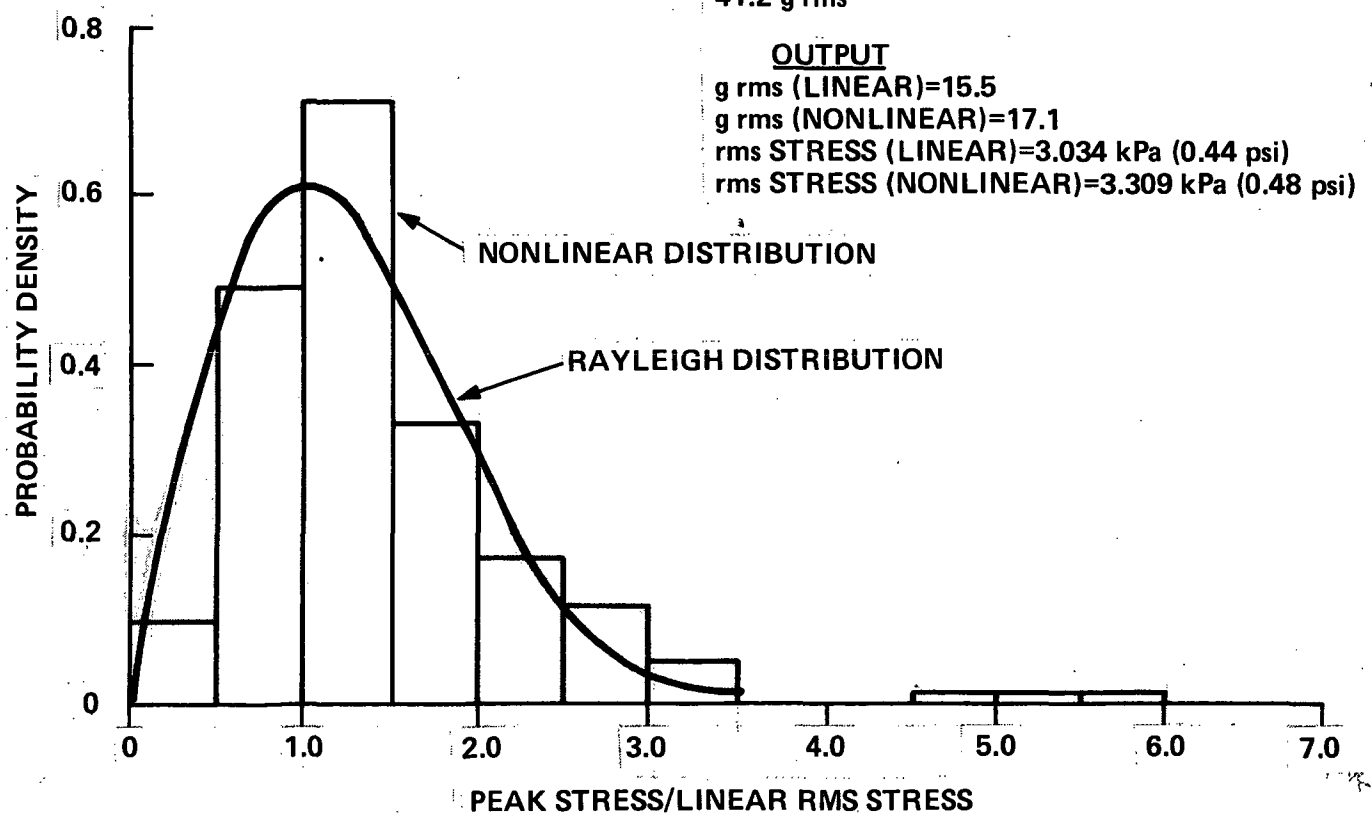


Figure 21. Comparison of Rayleigh and Nonlinear Probability Distribution Predictions for Peak Positive Pad Stress (Heavy Tile -  $1 \text{ g}^2/\text{Hz}$  ).

**TILE WEIGHT = 0.3186 Kg (0.7025 LB)**  
**PAD AREA = 161.3 cm<sup>2</sup> (25 IN.<sup>2</sup>)**  
**PAD THICKNESS = 0.4064 cm (0.160 IN.)**

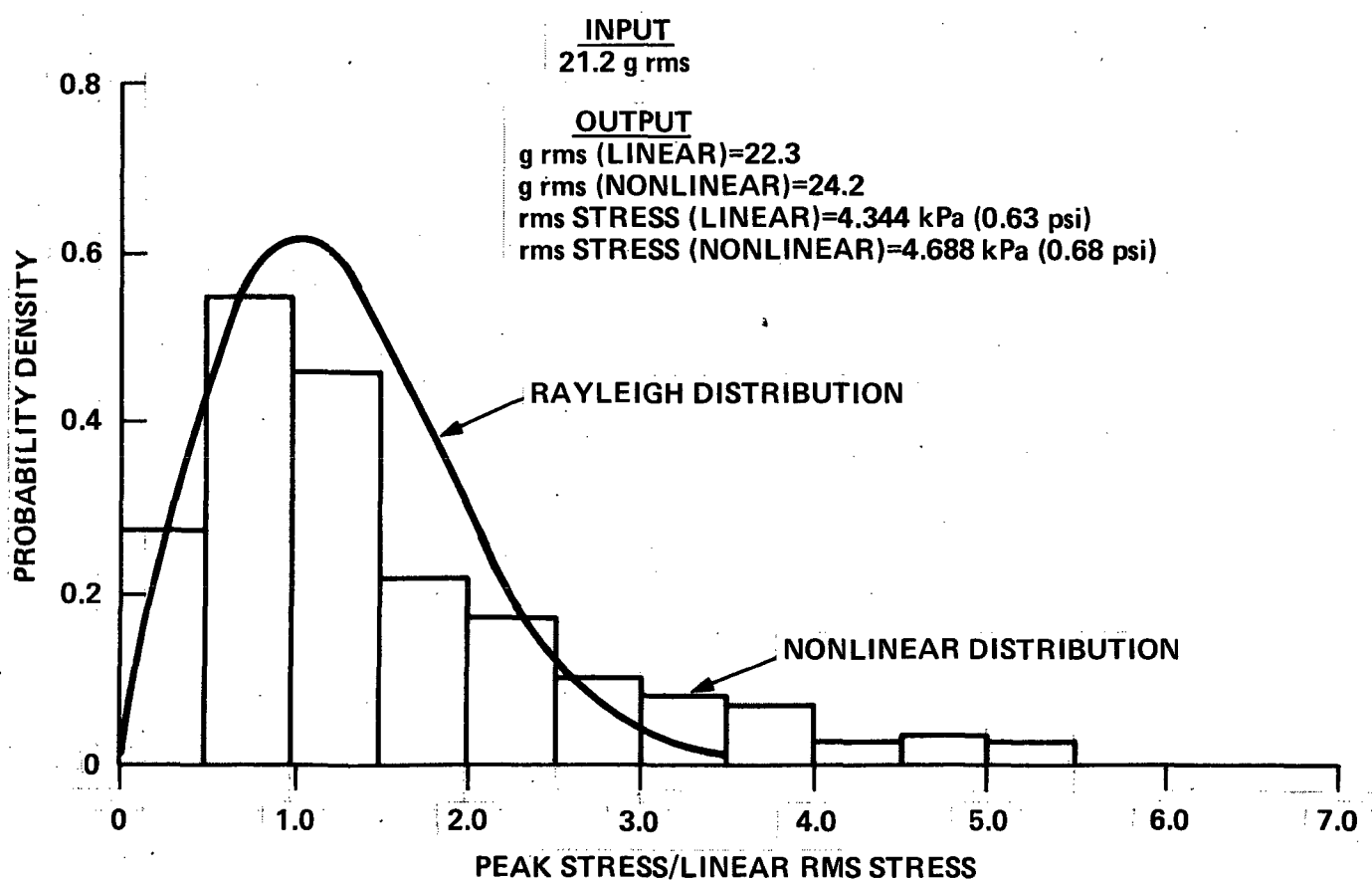
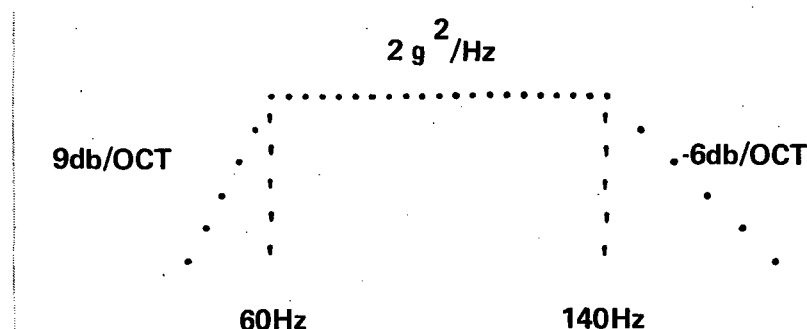


Figure 22. Comparison of Rayleigh and Nonlinear Probability Distribution Predictions for Peak Positive Pad Stress (Heavy Tile -  $2 \text{ g}^2/\text{Hz}$ ).

**TILE WEIGHT = 0.3186 Kg (0.7025 LB)**  
**PAD AREA = 161.3 cm<sup>2</sup> (25 IN.<sup>2</sup>)**  
**PAD THICKNESS = 0.4064 cm (0.160 IN.)**

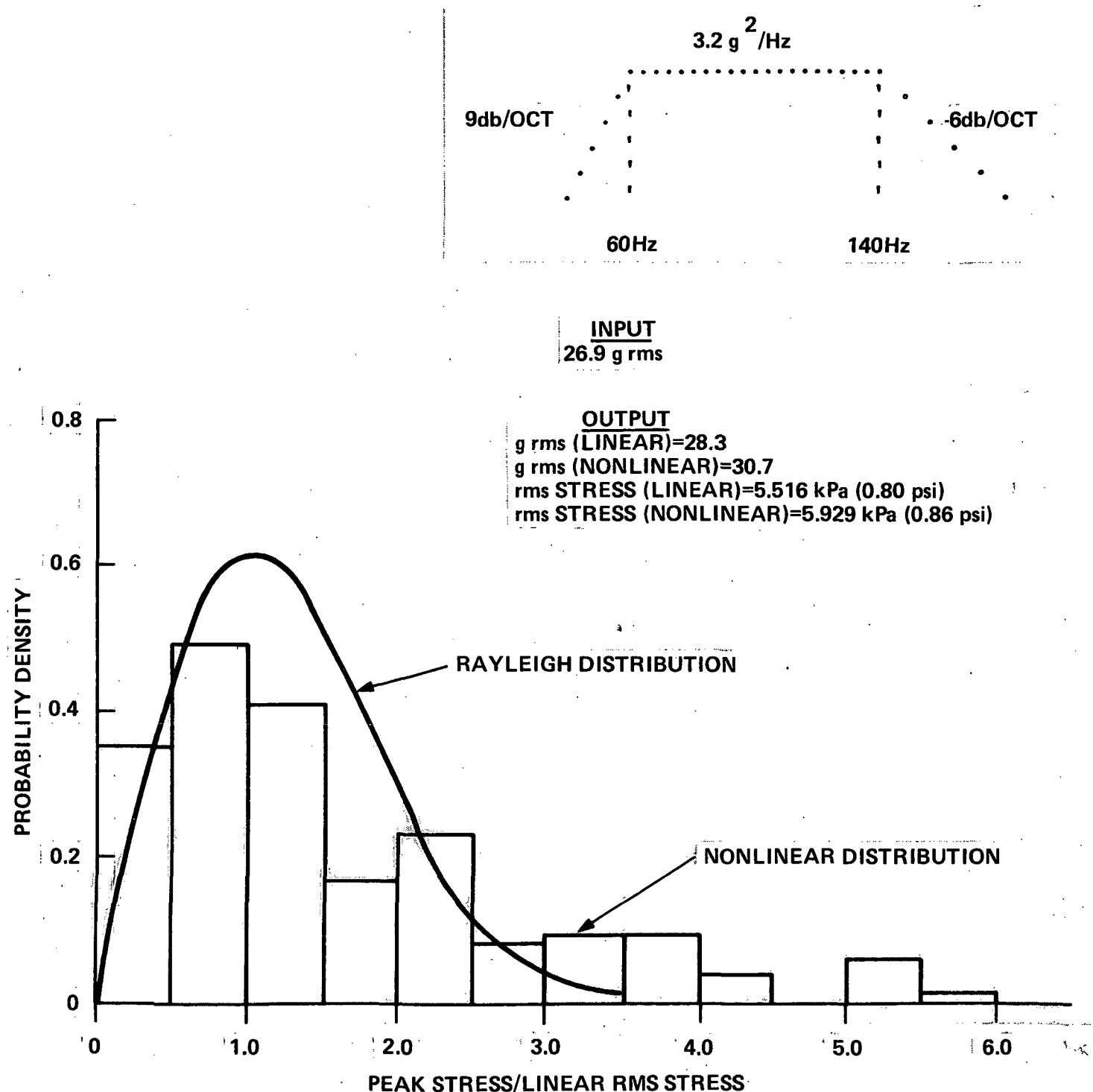


Figure 23. Comparison of Rayleigh and Nonlinear Probability Distribution Predictions for Peak Positive Pad Stress (Heavy Tile -  $3.2\text{g}^2/\text{Hz}$ ).

TILE WEIGHT=0.3186 Kg (0.7025 LB)  
 PAD AREA=161.3 cm<sup>2</sup> (25 IN.<sup>2</sup>)  
 PAD THICKNESS=0.4064 cm (0.160 IN.)

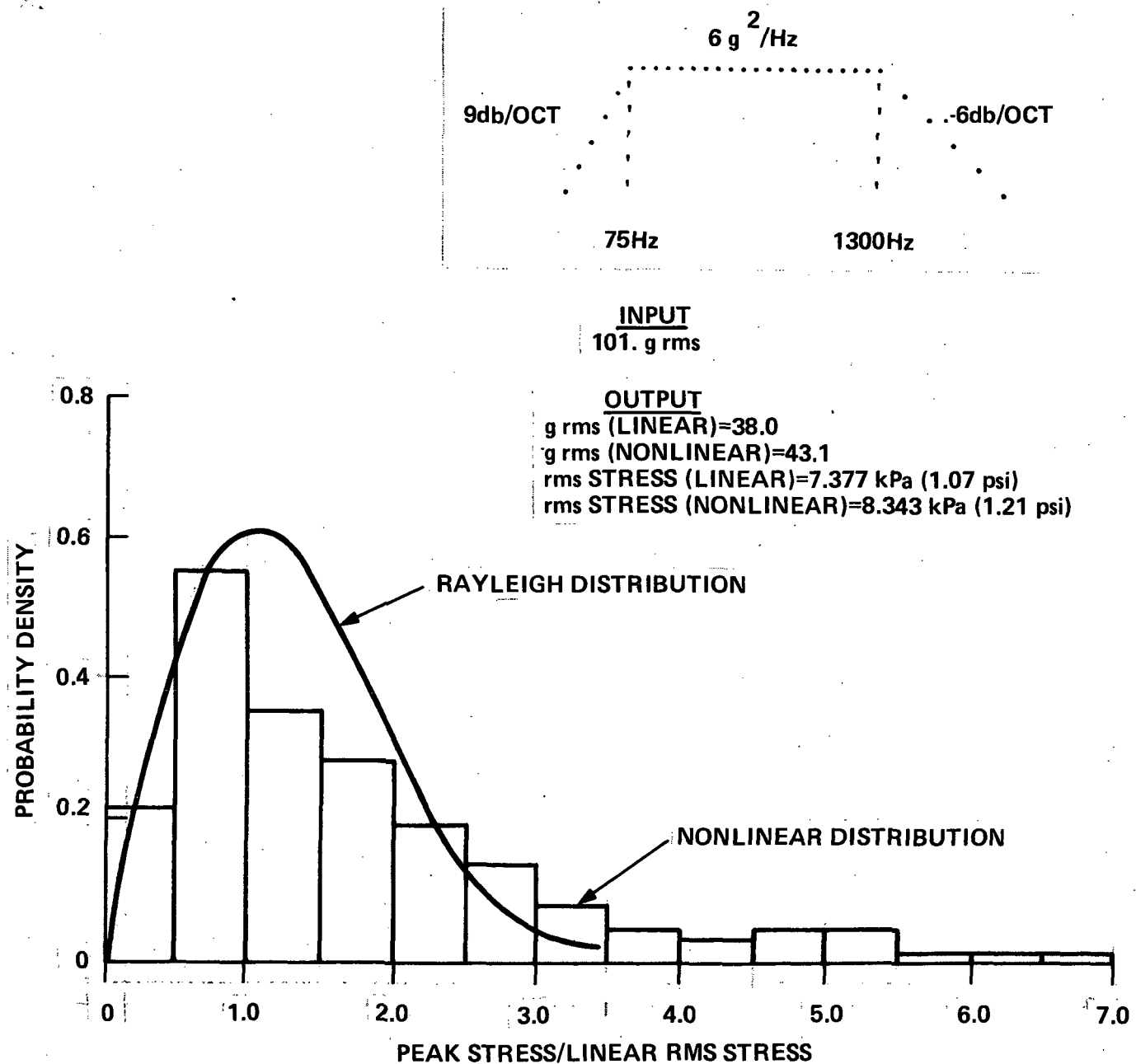


Figure 24. Comparison of Rayleigh and Nonlinear Probability Distribution Predictions for Peak Positive pad Stress (Heavy Tile ~  $6\text{g}^2/\text{Hz}$ ).

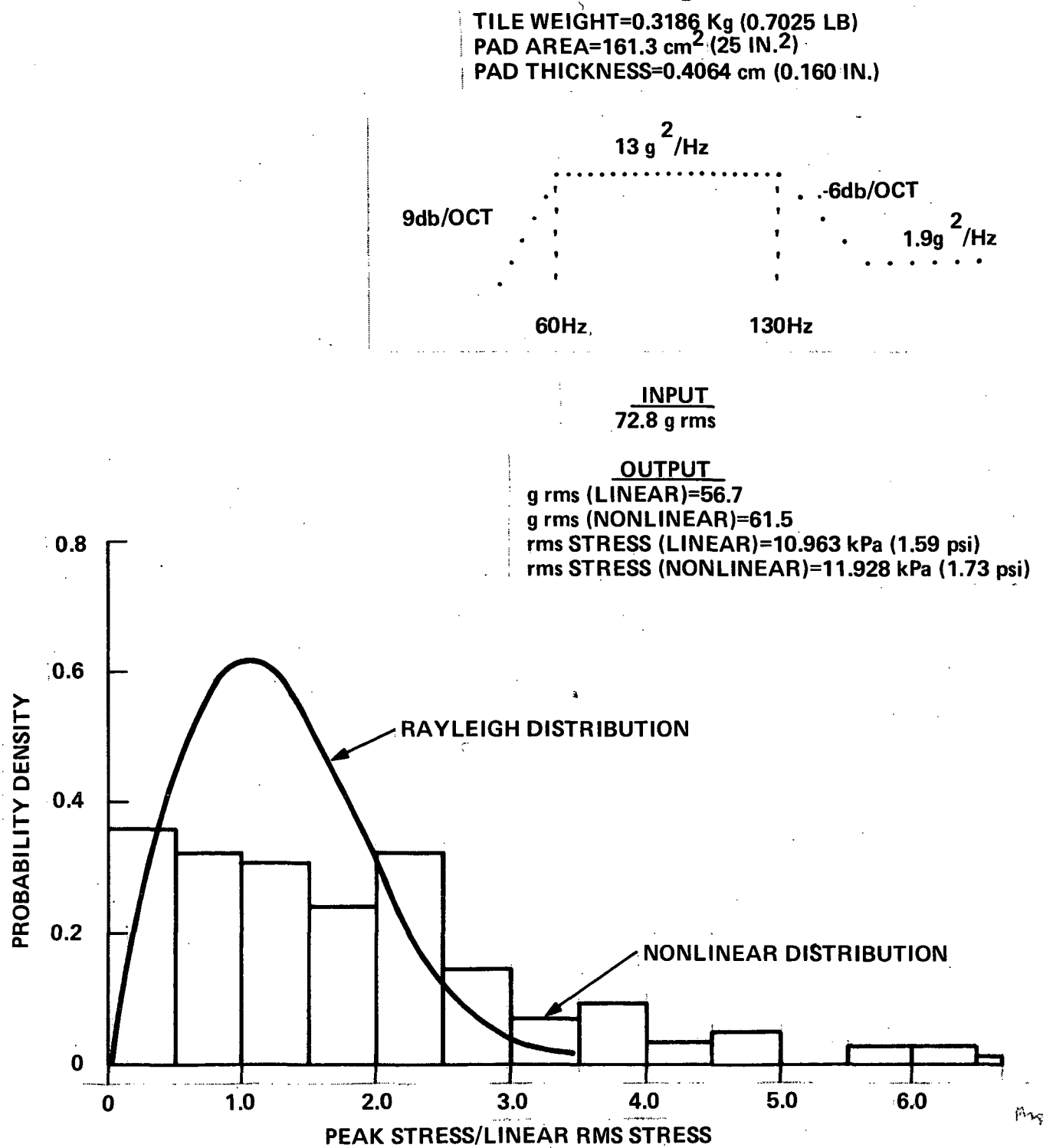


Figure 25. Comparison of Rayleigh and Nonlinear Probability Distribution Predictions for Peak Positive Pad Stress (Heavy Tile -  $13\text{g}^2/\text{Hz}$ ).

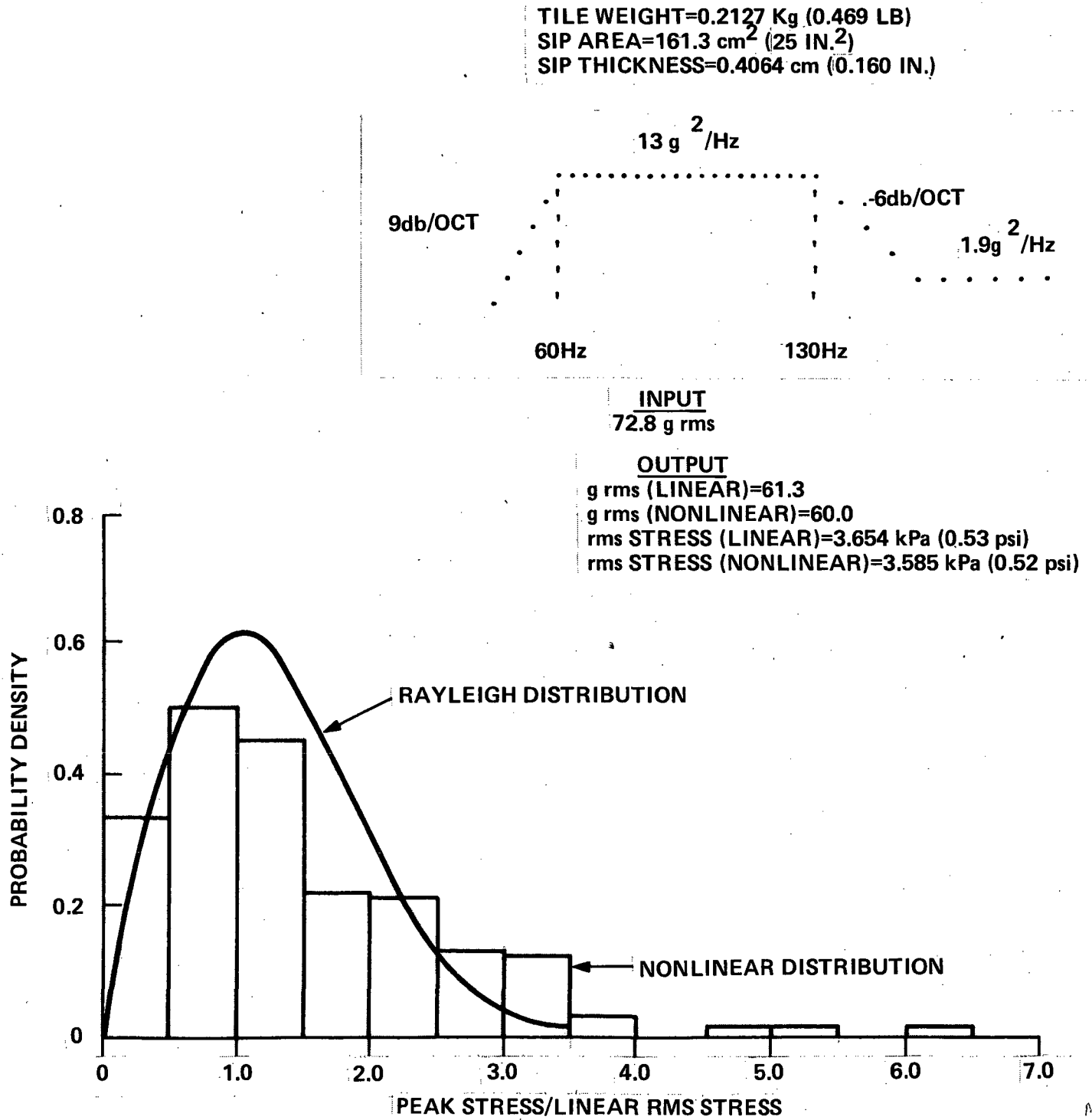


Figure 26. Comparison of Rayleigh and Nonlinear Probability Distribution Predictions for Peak Positive Pad Stress (Medium Weight Tile -  $13\text{g}^2/\text{Hz}$ ).

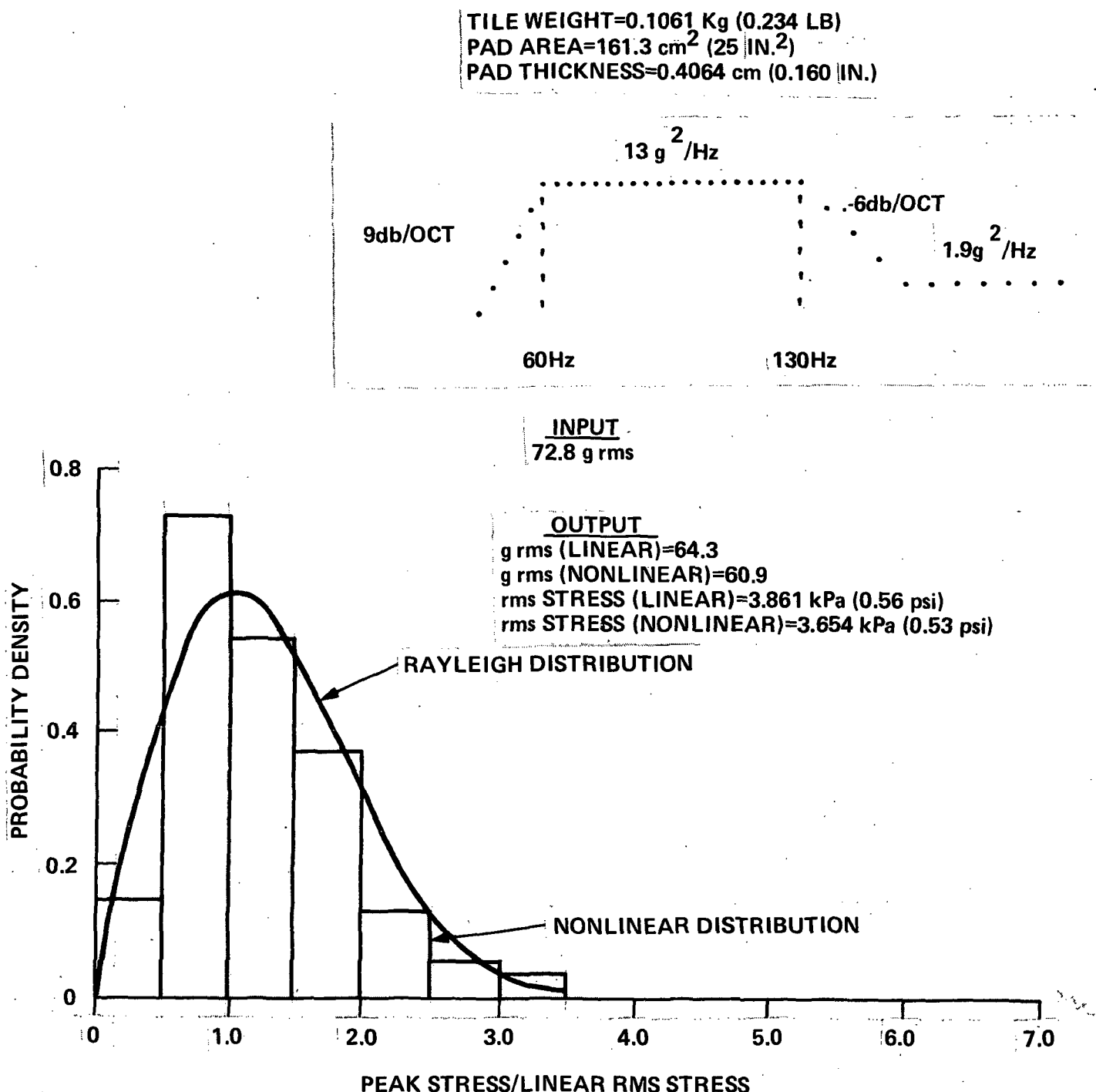


Figure 27. Comparison of Rayleigh and Nonlinear Probability Distribution Predictions for Peak Positive Sip Stress (Lightweight tile -  $13 \text{ g}^2/\text{Hz}$  ).

## Sensitivity of Analytical Prediction to Pad Material Conditioning

As reported in reference 3, the stress-strain law for the pad depends upon the number of and amplitude of load cycles the material has experienced. These cycles tend to condition the material. Conditioning may be accounted for approximately through the use of a material parameter,  $f_{\epsilon}$ , defined and discussed in reference 3. In addition  $f_{\epsilon}$  will also vary as a result of scatter in material properties from specimen to specimen. The sensitivity of tile response to this factor is considered in this section. The value of the material strain factor,  $f_{\epsilon}$ , was varied in the analysis using values of 0.6, 0.8 and 1.0. The value of 1.0 was used for all of the parametric curves in previous sections. With  $f_{\epsilon}$  equal to 1.0, the stress strain envelope of the pad material used, is the one shown in Figure 2. When a value of .8 is used, all of the strain dimensions are reduced to 80 percent with the stress dimensions being unchanged. This in effect increases the stiffness of the pad material. With a value of .6, the strains are reduced to 60% of the basic envelope values. All of the internal curved paths are changed because they are given the same shape as the outer envelope. The parametric study was carried out using the properties tabulated in Table 1. The test data was performed on a square LI 900 tile on a .437 cm (.172 in.) pad as previously described. The pad area, tile area, pad thickness, and the structural mass in Table 1 were used in the analysis. Substrate acceleration tests and analysis were performed and the resonant frequency and magnification factor comparison plotted in Figures 28 and 29. From this data in Figure 28 and 29 it is concluded that a value of .7 to .8 for  $f_{\epsilon}$  agreed best with test data. Tests were also performed with a constant 12g substrate acceleration with variations in the steady outboard pressure on the tile. The correlation of nonlinear analysis and test data is shown in Figure 30. This data indicates that a value near .8 should be used for  $f_{\epsilon}$ . If the parametric curves presented in previous sections had used a value of .8 the frequencies would be 10 to 15 Hz higher and the magnification factors would be higher by about 40% when the substrate amplitude is above 20.

For random nonlinear analysis, as reported in the following section, the value of .7 for  $f_{\epsilon}$  is recommended.

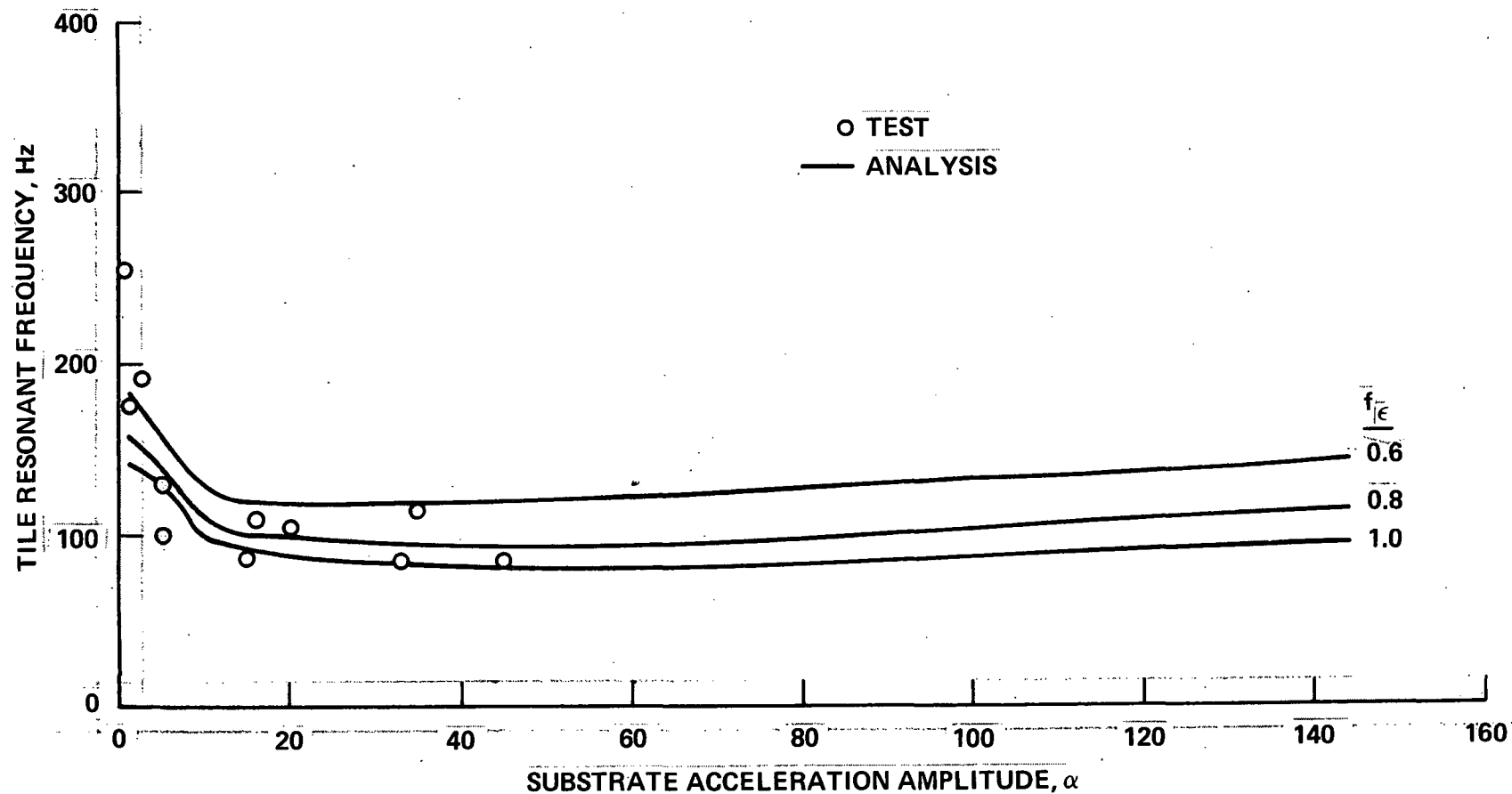


Figure 28. Sensitivity of Tile Resonant Frequency in the Absence of Tile Steady Pressure to Pad Material Conditioning Factor,  $f_{\epsilon}$ .

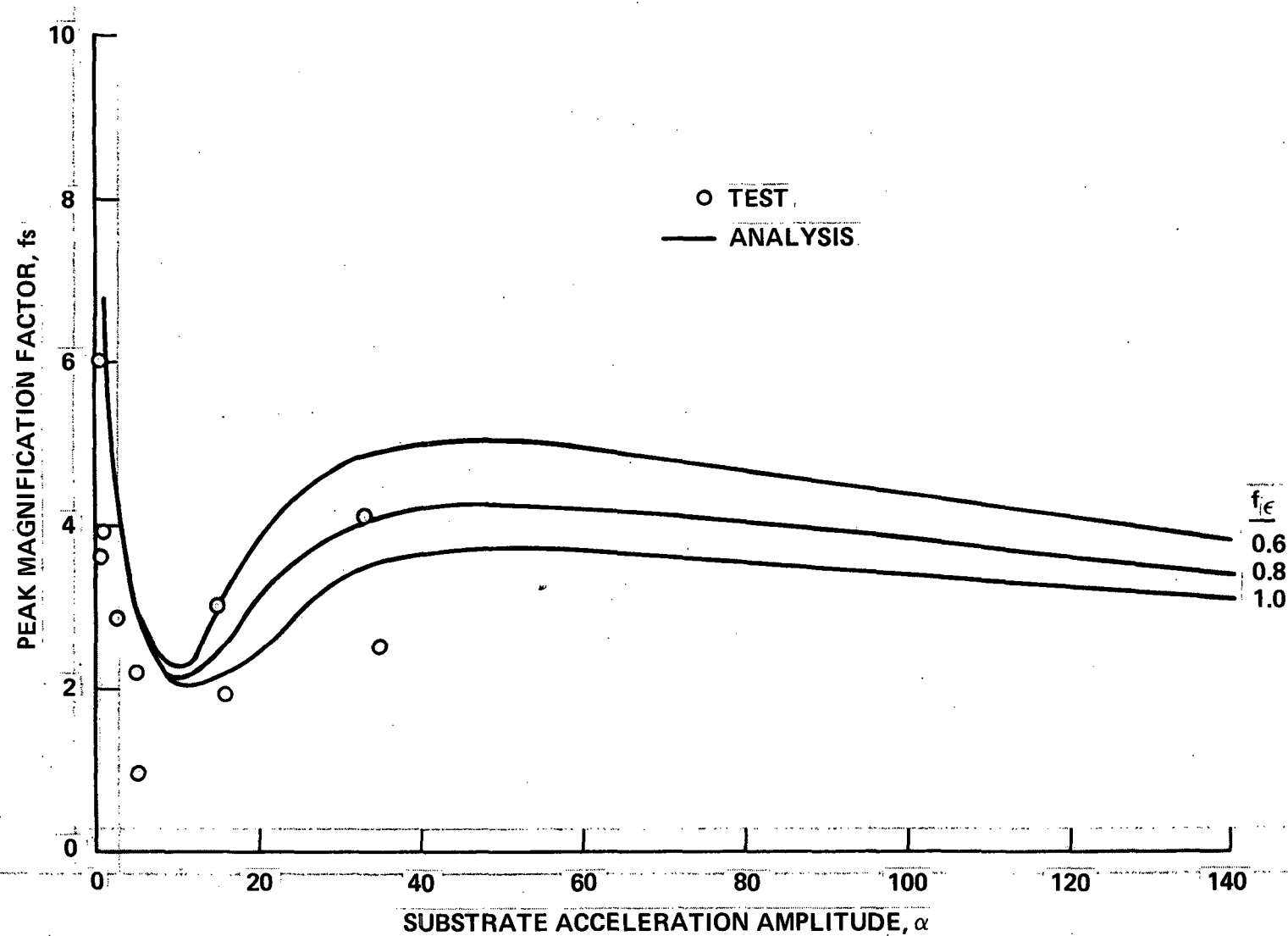


Figure 29. Sensitivity of Tile Peak Magnification Factor to Pad Material Conditioning Factor,  $f_{\bar{\epsilon}}$ .

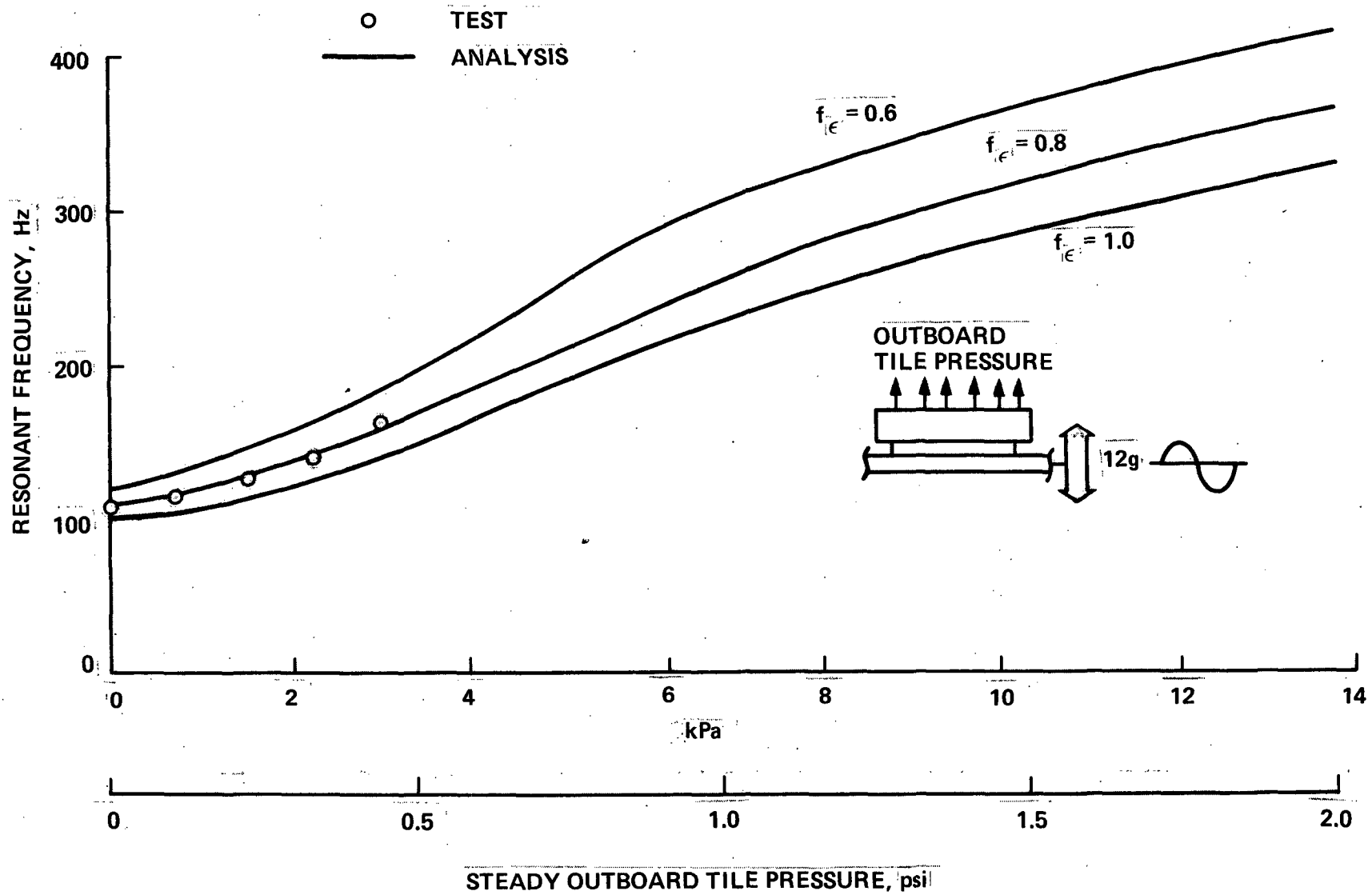


Figure 30. Sensitivity of Tile Resonant Frequency in the Presence of Steady Tile Pressure to Pad Material Conditioning Factor,  $f_{\epsilon}$ .

Comparison of Test and Nonlinear Analysis  
for Random RMS and Peak Output/Input Acceleration

Random spectral tests and nonlinear analysis were performed at different substrate peak  $\text{g}^2/\text{Hz}$  levels on .454 and .844 Kg (1.0 and 1.86 pound) tile/pad configurations. The test and analysis rms and peak tile-acceleration/substrate-acceleration ratio was determined and plotted against the substrate rms acceleration level in Figure 31. The .454 Kg (1.86 lb) tile mass is high for a typical shuttle tile but was selected specifically for test-analysis correlation. In performing this random nonlinear analysis it was determined that the best correlation was obtained when the material strain factor,  $f_\epsilon$ , of 0.7 was used.

The analysis-test correlation was very good for the tile-rms-acceleration/substrate-rms-acceleration ratio except at very low input rms acceleration levels. The peak stress output/input ratios also show better correlation at the higher input rms acceleration levels.

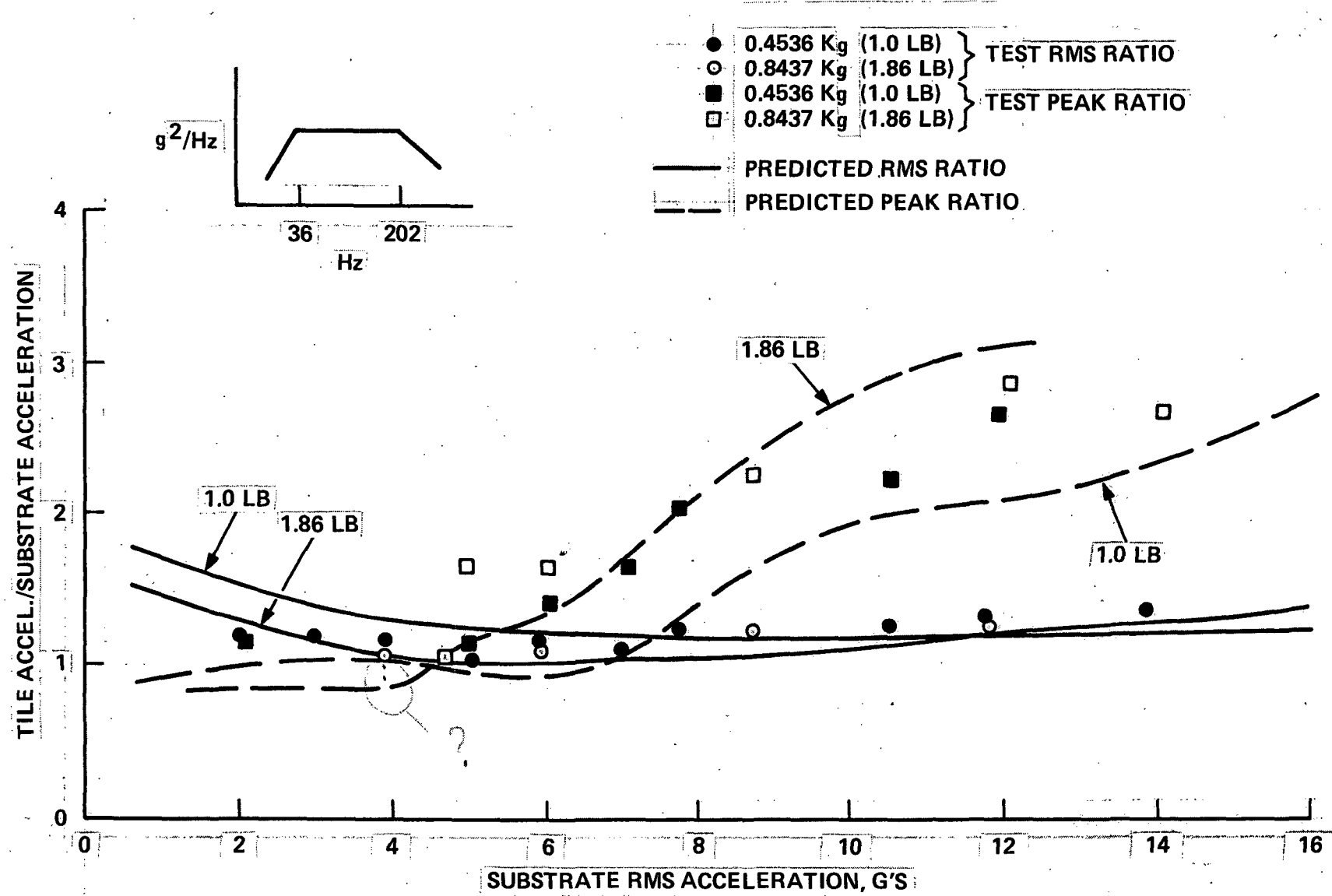


Figure 31. Comparison of Test and Nonlinear Analysis for rms and Peak Acceleration.

## TILE MASS EFFECTS

The parametric curves were all performed on a square LI 900 tile with a mass of .3187 Kg (.00182 lb-sec<sup>2</sup>/in) as shown in Figure 1. To determine the mass effect on the pad stress, the mass was varied from .04377 to .6653 Kg (.00025 to .0038 lb/sec<sup>2</sup>/in) with an oscillating tile pressure of 4.785 kPa (.694 psi). The pad stress variation with change in input frequency is shown in Figure 32. The resonant frequency decreases with increasing mass but at a slower rate than a linear system as shown in Figure 33. On this type of plot all linear moduli systems would be straight lines parallel to the one shown for a linear system with a pad Young's Modulus of 15. Analysis was also performed with mass variations for a 60 g substrate sinusoidal acceleration with the resulting resonant frequencies plotted in Figure 33. For low mass tiles the resonant frequency change is linear in nature, but exhibits the nonlinear characteristics for heavier tiles. The oscillating substrate and pressure curves have different shapes because the fixed amplitude substrate motion is equivalent to an increasing tile load as the mass is increased.

To determine the change in the maximum pad stress with changes in mass, the pad stress multiplying factor,  $m_s$ , is

$$m_s = \frac{\sigma}{\sigma_0} \quad (7)$$

where

$\sigma$  is the stress due to a given tile mass

$\sigma_0$  is the stress due to the LI 900 tile mass of .3187 Kg (.00182 lb-sec<sup>2</sup>/in).

The variation of the pad stress multiplying factor with tile mass is shown in Figure 34 for the 60 g substrate acceleration and for the 4.785 kPa (.694 psi) sinusoidal tile pressure case. As the tile mass is increased, the pad response stress increases at a faster rate for substrate sinusoidal acceleration than for sinusoidal tile pressure vibrations.

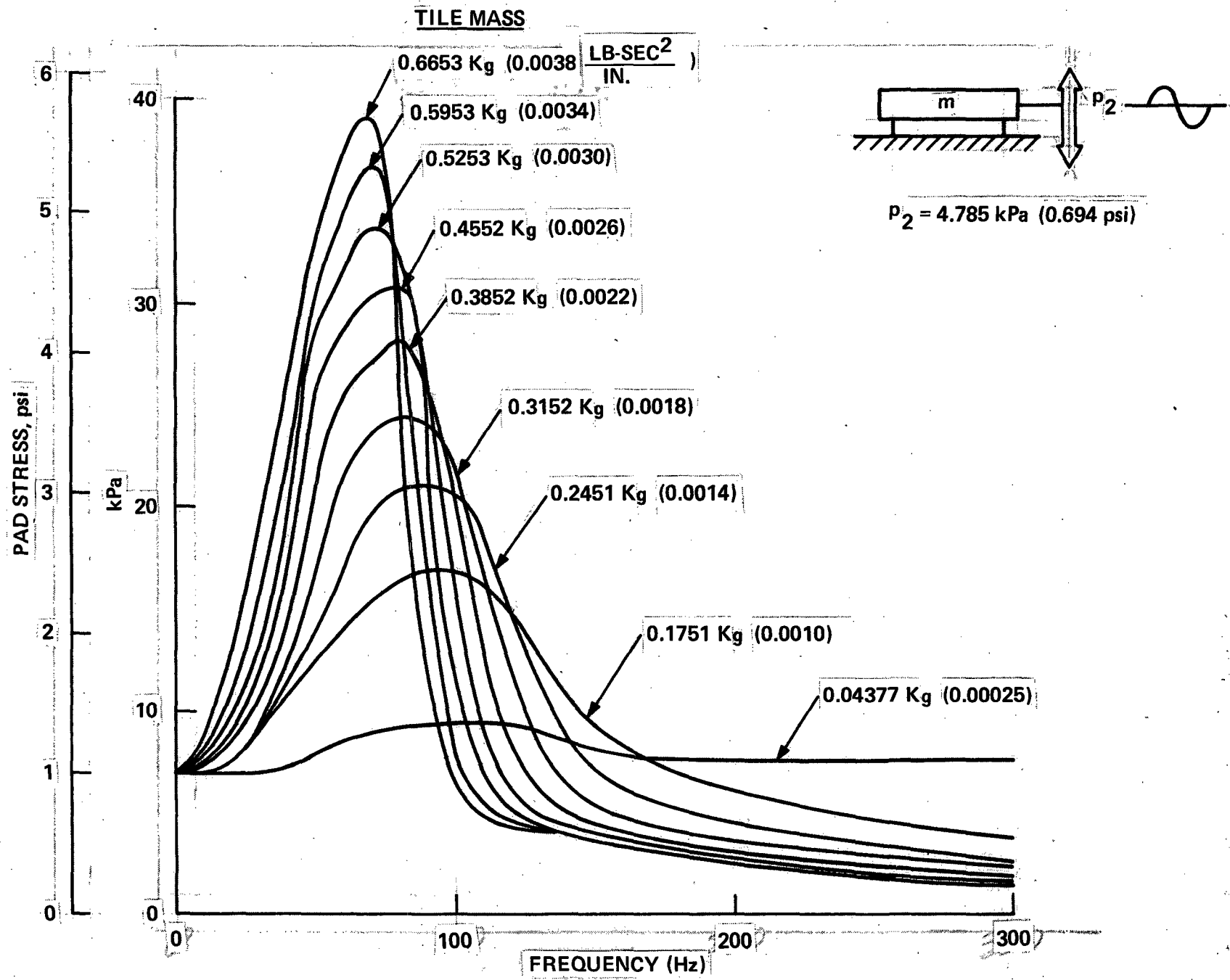


Figure 32. Effect of Tile Mass on Pad Stress For Oscillating Pressure of 4.785 kPa (0.694 psi).

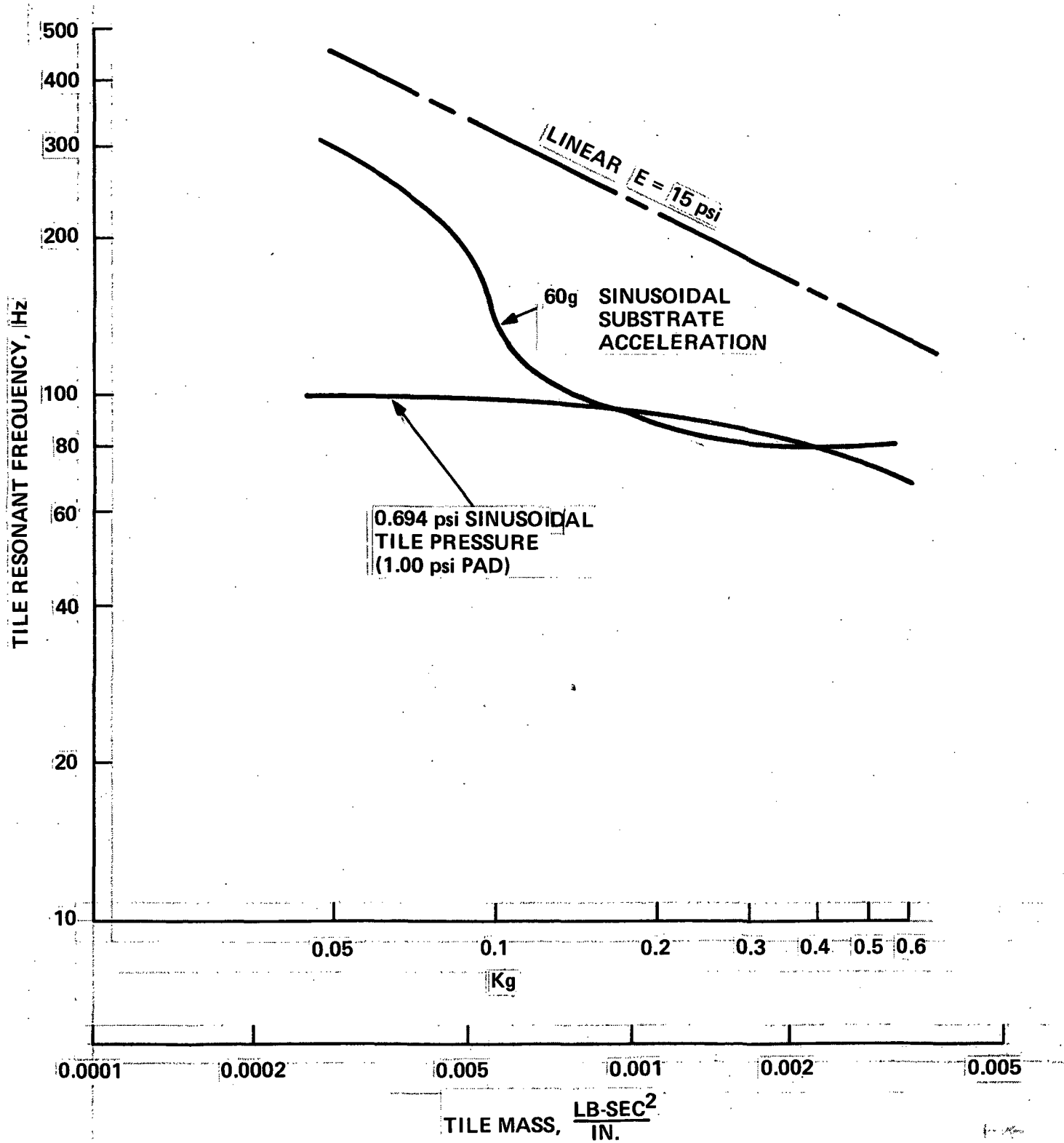


Figure 33. Effect of Tile Mass on Tile Resonant Frequency.

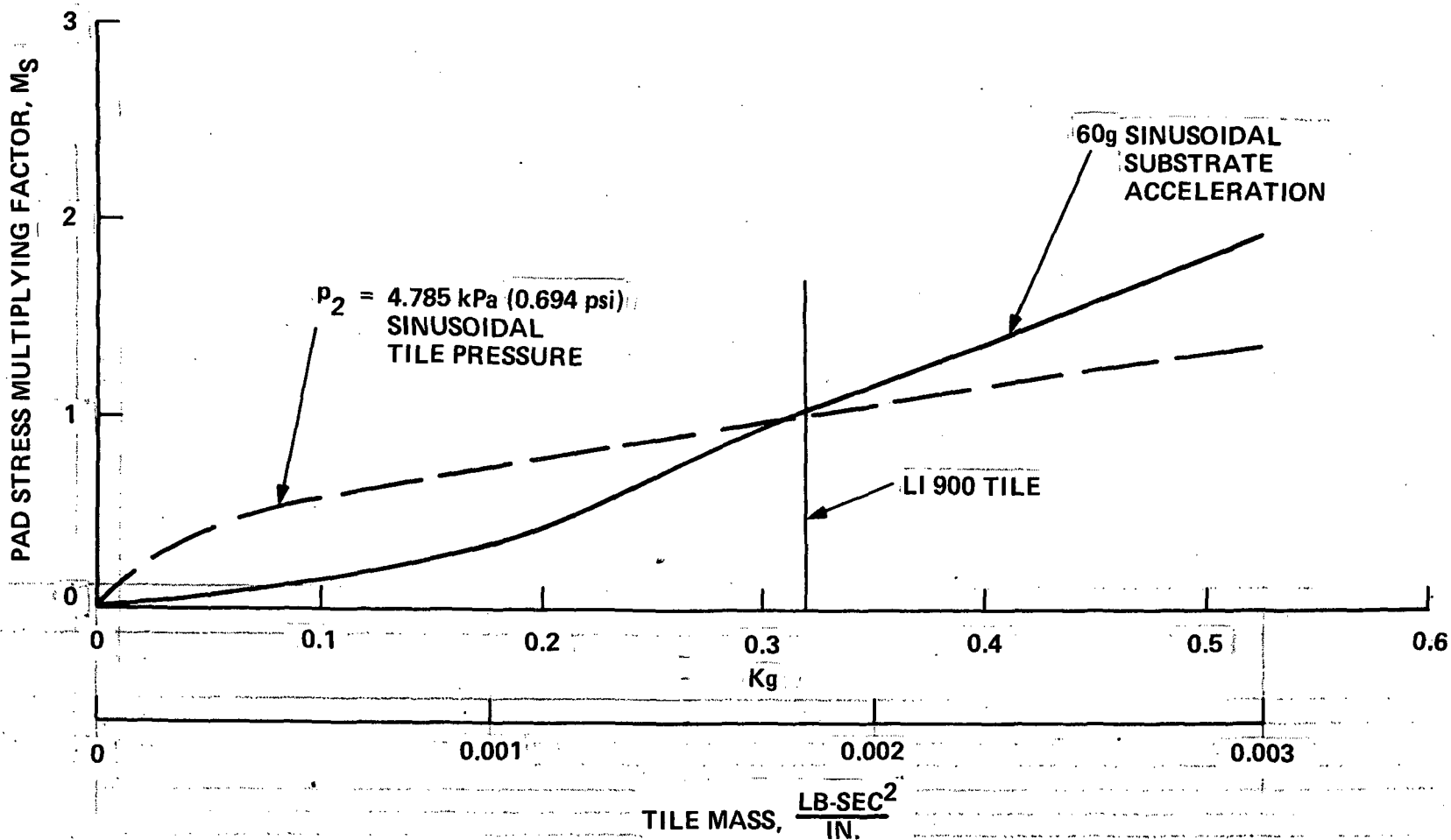


Figure 34. Variation of Pad Stress Multiplying Factor With Tile Mass.

## CONCLUDING REMARKS

The nonlinear dynamic response of the space shuttle tile/pad thermal protection has been studied using the nonlinear computer code of reference 3. Parametric studies were performed on a typical LI 900 tile with subsequent evaluation of tile mass effects. Thus, the approximate response of any tile subjected to oscillating tile pressure or substrate acceleration in the presence of a steady tile pressure can be evaluated. The following remarks summarize the findings of these studies:

1. The most important aspect of combining a steady pressure with the sinusoidal tile pressure or substrate oscillation, is that the pad maximum response stress changes significantly more than the applied steady pressure. In the presence of a steady tile differential pressure inboard the peak pad stress decreases 5 times the steady pressure. In the presence of a steady outboard pressure less than -6.89 kPa (-1.00 psi) the peak pad stress increases approximately twice the steady pressure. For further increases in outboard steady pressure the trend reverses and the peak pad stress decreases.
2. The resonant frequency decreases with increasing tile mass but at a different nonlinear rate when compared to a linear system. When the tile is excited by a sinusoidal pressure, the resonant frequency decreases at a much slower rate than a linear system as the tile mass is increased. When there is a substrate sinusoidal acceleration, the resonant frequency change is linear in nature for low mass tiles, but exhibits very nonlinear characteristics for heavier tiles.
3. Pad material properties vary from specimen to specimen and in addition depend on the number and level of conditioning cycles experienced by the pad during its previous history. It has generally been found that as a consequence most specimens

used for comparison could be adequately modeled using a conditioning factor,  $f_{\epsilon}$ , of .7 to .8. A value of 0.8, versus the 1.0 value used in the parametric evaluation, results in a stiffer pad material. Relative to the results with  $f_{\epsilon}=1$ , this change will result in increases of resonant frequencies of 10 to 15 Hz and a 40% increase in magnification factors or peak pad stresses.

4. Comparing test and nonlinear random analysis of the RMS and peak acceleration levels, indicates that the nonlinear analysis correlates very well with test data. The RMS analysis accelerations were very close to the RMS test accelerations except at the very low substrate spectral input levels where the analysis was slightly below the test RMS acceleration levels. At the moderate to high substrate accelerations where the magnitude of pad stresses become important to the integrity of the system, the analysis-test correlation was very good. A material conditioning factor,  $f_{\epsilon}$ , of .7 was used to obtain this correlation.
5. Comparison of linear and nonlinear predicted probability of occurrence for positive peak pad stresses due to random Gaussian substrate accelerations indicated that the linearly predicted RMS stress value is reasonably accurate. However, due to nonlinearities in the system, the Rayleigh distribution does not provide an adequate probability of occurrence prediction for high stress peaks and thus the use of a "3-SIGMA" value may be unconservative. It is recommended that a factor higher than 3 on linearly predicted stress be used except for very lightweight tiles. For the heaviest tiles a factor of 6 is recommended independent of the level of substrate motion. For moderately heavy tiles this can be reduced depending on the level of the substrate motion, but it does not appear that a general statement on the factor to be used can safely be made. For the very light tiles, a factor of 3 (i. e. the 3-SIGMA value) seems to be acceptable.

6. Charts are provided for determining peak pad stress and system resonant frequencies.
  - a. For a LI 900 tile, the pad stress can be found for a specific sinusoidal tile pressure and combined steady pressure by using Figures 3, 4, 5 and 6.
  - b. For a LI 900 tile, the pad stress can be found for a specific sinusoidal substrate acceleration and combined steady tile pressure by using Figures 10, 11, 12 and 13.
  - c. If the maximum pad stress is desired for a LI 900 tile at resonant frequency for a specific substrate acceleration amplitude or a tile sinusoidal tile pressure amplitude combined with a steady tile pressure, use Figure 14.
  - d. If the tile resonant frequency is desired for a LI 900 tile for the conditions in item c above, use Figure 15.
  - e. If the maximum magnification factor is desired for a LI 900 tile at resonant frequency for the conditions in item c above, use Figure 16.

## REFERENCES

1. Sawyer, J. W.; and Rummler, D. R.: Room Temperature Mechanical Properties of Shuttle Thermal Protection Systems Materials. NASA TM-81786, April 1980.
2. Housner, J. M.; and Garcia, R.: Nonlinear Static TPS Analysis. NASA TM-81785, March 1980.
3. Housner, J. M.; Edighoffer, H. H; and Park, K. C.: Nonlinear Dynamic Response of a Uni-directional Model for the Tile/Pad Space Shuttle Thermal Protection System. NASA TM-81901, November 1980.
4. Miserentino, R.; Pinson, L. D.; and Leadbetter, S. A.: Some Space Shuttle Tile/Strain-Isolator-Pad Sinusoidal Vibration Tests. NASA TM-81853, July 1980.
5. Miserentino, R.; Pinson, L. D.; and Leadbetter, S. A.: Some Vibration Characteristics of a Space Shuttle Tile/Strain-Isolator-Pad System. Presented at the 1980 SAE Aerospace and Exposition, Oct. 13-16, 1980, Los Angeles, CA.

## **APPENDIX**

62

## EFFECT OF LOADING/UNLOADING LOOP PARAMETERS

In this appendix the effect of the stress-strain loading/unloading loop parameters  $\beta$  and  $\gamma$  as defined in reference 3 is discussed.

When the tile motion traces out a loop lying entirely within the range  $\bar{\epsilon}_L \leq \epsilon \leq \bar{\epsilon}_U$ , the loop consists of a curved loading and curved unloading path as shown in View A of Figure 2 and  $\beta$  as defined in equations (2) and (3) is ineffective. The  $\beta$  parameter only affects the position of a loop which extends outside of this range giving the loop a straight loading or unloading path whose slope is  $E_L$  or  $E_U$ .

The low stress factor,  $\gamma$ , as defined in reference 3 is effective in the region between  $\bar{\epsilon}_L$  and  $\bar{\epsilon}_U$ , and only when the input load amplitude is low so that the equilibrium loop does not extend to both the upper and lower boundaries of the hysteretic envelope. This condition is shown in View A of Figure 2. A value of  $\gamma$  that is less than unity will result in steeper fifth order polynomial curves resulting in higher frequencies and magnification factors at very low input amplitudes.

The low stress factor,  $\gamma$ , and the multiplying factor,  $\beta$ , were set equal to the default values of 0.5 and 2 at the start of the parametric study but in some cases the computer run time to obtain equilibrium response became excessive. To circumvent this problem, the value of  $\gamma$  was set equal to 1.0 and the value of  $\beta$  was set equal to 100 for the parametric evaluation. The value of  $\gamma$  equal to 1.0 results in tile resonant frequencies that are lower than test data at very low substrate acceleration levels. As shown in Figure 28, when the substrate acceleration amplitude,  $\alpha$ , is less than 5, the analysis predicts lower frequencies than the test data. Experience has shown that the response is insensitive to the value of  $\gamma$  when substrate acceleration amplitude is 10 or greater or when the tile sinusoidal pressure is 1.72 kPa (.25 psi) or greater. The high value of  $\beta$  used, results in a small reduction in the maximum stress and a small reduction in the indicated resonant frequency when compared with the default value of 2.

1. Report No. NASA 165707	2. Government Accession No.	3. Recipient's Catalog No.	
4. Title and Subtitle PARAMETRIC ANALYTICAL STUDIES FOR THE NONLINEAR DYNAMIC RESPONSE OF THE TILE/PAD SPACE SHUTTLE THERMAL PROTECTION SYSTEM		5. Report Date October 28, 1981	
7. Author(s) Harold H. Edighoffer		6. Performing Organization Code	
9. Performing Organization Name and Address General Electric Company, Re-entry Systems Division 3198 Chestnut Street Philadelphia, PA 19101		8. Performing Organization Report No.	
12. Sponsoring Agency Name and Address NASA Langley Research Center Hampton, VA		10. Work Unit No.	
		11. Contract or Grant No. NASI 16121	
		13. Type of Report and Period Covered Contractor report	
		14. Sponsoring Agency Code	
15. Supplementary Notes			
16. Abstract			
<p>This paper presents a collection of parametric unidirectional analytical studies of the nonlinear dynamic behavior of the space shuttle tile/pad thermal protection system for imposed sinusoidal and random motions of the shuttle skin and/or applied tile pressure. The analysis accounts for the highly nonlinear stiffening hysteresis and viscous behavior of the pad which joins the tile to the shuttle skin. Sinusoidal and random experimental data are used to confirm the validity of the analysis. With no steady pressure on the tile, the system resonant frequency is very high at low amplitude oscillations and decreases rapidly to a minimum value with increased amplitude. When a steady tile pressure in the outboard direction is superimposed on the oscillating input, the resonant frequency increases to very high values while inboard steady pressures decrease the frequency. The inboard steady pressure decreases the maximum tensile pad stress about five times the amount of the steady pressure applied. On the other hand, outboard steady pressure on the tile results in increased maximum tensile pad stress two times the amount of the applied steady pressure until the steady pressure reaches 6.89 kPa (1.0 psi), which is the point of maximum pad stress. Beyond this value the pad stresses decrease with further increase in outboard steady pressure.</p>			
17. Key Words (Suggested by Author(s)) Space Shuttle Dynamics Structure      Thermal Protection System		18. Distribution Statement Unclassified	
19. Security Classif. (of this report) Unclassified	20. Security Classif. (of this page) Unclassified	21. No. of Pages 71	22. Price